Journal of Nonlinear Modeling and Analysis
Volume 7, Number 3, June 2025, 946–986
https://journal.global-sci.org/jnma
DOI:10.12150/jnma.2025.946

Optimal Control of a Delayed Spatiotemporal Epidemic Model

Amine Alabkari[1,†], Ahmed Kourrad[1], Khalid Adnaoui[1] and Hassan Laarabi[1]

Abstract This study presents an advanced delayed spatiotemporal epidemiological model that incorporates a Holling type II incidence rate to capture the saturation effects observed in disease transmission dynamics during the COVID-19 pandemic. The model integrates two crucial intervention measures - vaccination of susceptible individuals and hospitalization of severe cases - while accounting for both spatial diffusion and the latent period within the epidemic compartments. This framework facilitates the precise optimization of vaccination and hospitalization strategies as functions of spatial location and temporal evolution, yielding new insights into spatially targeted public health interventions. We rigorously analyze the model equilibrium points, establishing conditions for their existence and local stability. An optimal control problem is formulated, uniquely considering the combined effects of spatial diffusion and latent period, with controls dynamically varying across space and time. The well-posedness of the control problem is verified, supported by proofs of existence, uniqueness, positivity, and boundedness of the strong solution. First-order necessary optimality conditions are derived, characterizing the optimal vaccination and hospitalization strategies through state and adjoint variables. Numerical simulations across diverse intervention scenarios demonstrate the effectiveness of adaptive, space-time-specific control strategies in mitigating COVID-19 transmission. This work offers a novel mathematical and computational approach to the optimal spatiotemporal management of epidemic control measures.

Keywords Delayed spatiotemporal epidemic model, vaccination, hospitalization, reaction-diffusion equations, optimal control

MSC(2010) 49-XX, 49K20, 92D30.

1. Introduction

With the emergence of epidemics like SARS, Ebola, and COVID-19, which are detrimental to individual health and societal stability, there is an increased need for policymakers and researchers to understand the patterns, the behaviors, and the dynamics of the diseases in order to prevent and control their spread. Mathematicians and immunologists collaborate to create models that can predict the course

[†]the corresponding author.
Email address: aminealabkari@gmail.com (A. Alabkari), ahmedkourrad@gmail.com (A. Kourrad), khalid.adnaoui@gmail.com (K. Adnaoui), hlaarabi@yahoo.fr (H. Laarabi)
[1]Laboratory of Analysis Modeling and Simulation, Faculty of Sciences Ben M'Sik, Hassan II University, BP 7955, Sidi Othman, Casablanca, Morocco.

of an epidemic. Classical compartmental models for epidemics use variables to describe the state of an infectious disease's exposed subpopulation. Each parameter incorporated represents a fundamental factor, such as the rate of transmission of the infectious agent, the mortality rate, and other data. It is possible to build very reliable models that will allow determining the best treatments as well as the respective impacts of the factors that influence this disease with a thorough knowledge not only of applied mathematics but also of the biology of the disease. These models are determined by the transmission method, the nature of the disease, its curability, and the body's ability to develop immunity after recovery, etc. [15, 18]. Following the 1905 - 1906 Bombay plague epidemic, the year 1927 witnessed the emergence of the SIR model, which is considered one of the first and most used compartmental models [20]. This model assumes that the population is divided into three subpopulations: susceptibles, infected, and recovered. Later, several compartmental models were inspired by the SIR and have been widely applied to research infectious disease outbreaks [10, 11, 18, 36, 44] and to examine potential policy responses. Since the COVID-19 outbreak, many authors have examined the dynamics of the disease's spread in light of various situations [14, 32, 35]. In particular, Ndaïrou et al. [32] presented a compartmental model of COVID-19 transmission dynamics with a case study of Wuhan where they focused on the transmissibility of superspreaders individuals. Samui et al. [35] proposed a compartmental mathematical model to predict and control the transmission dynamics of COVID-19 pandemic in India. They performed local and global stability analysis for the infection free equilibrium point and the endemic equilibrium point with respect to the basic reproduction number. Diagne et al. [14] formulated and analyzed a mathematical model of COVID-19 transmission incorporating two key therapeutic measures: vaccination of susceptible individuals and treatment of infected individuals. In their model, they included a compartment (E) for exposed persons, responsible for the incubation period. For a model in which the size of the problem is relevant, It is preferable to attain the same dynamics with fewer compartments for a model. The dynamics won't, however, be exactly the same if a compartment (like E) is removed. In fact, we think that the formulation of the delay equation could better capture the effect of "delay" brought on by the introduction of new measures (as was the case with the COVID-19 pandemic), where there is a delay of several days between the introduction of a new public health order and when its effects start to be noticed. Additionally, delays may vary according to the stage of the epidemic, resulting in state-dependent delays. Although we won't look at such a case here, it is important to first grasp the case of constant delay, which is what this present effort is trying to do. Furthermore, from a mathematical perspective, such a formulation is intriguing. Several authors have reflected on this matter by studying the existence of solutions and bifurcations of time-delayed compartmental models [7, 19, 24, 27]. Furthermore, many studies seek the most effective strategy for reducing infection rates while minimizing implementation costs [9, 25]. However, all these works didn't take into consideration the spatial diffusion that is crucial to the propagation of epidemics and must be taken into account when implementing control strategies (for instance, an area that containts more infected individuals needs more attention). As a result, some authors [2–5, 16, 21, 22] investigated spatiotemporal models in which the disease spread was represented as a system of reaction-diffusion equations. However, to our knowledge, no deterministic model has treated an optimal control problem that takes into consideration simultaneously the spatial diffusion

and time delay in state variables. Incorporating delays and spatial diffusion allows for a more realistic representation of disease spread, as COVID-19 transmission is influenced not only by time-dependent processes (e.g., latent periods, temporary immunity) but also by spatial factors such as population movement and geographical clustering. Delayed models account for the latency period between infection and the onset of symptoms or infectiousness, which is crucial for modeling real-world disease spread and intervention timing [23]. The delay helps align the model with real epidemiological progression, as studies indicate that latent period impacts disease dynamics [18]. Ignoring delays would lead to an unrealistic representation, especially for diseases like COVID-19. Furthermore, this spatial-temporal approach enables us to optimize control measures like vaccination and hospitalization based on both position and time, offering practical insights into spatially adaptive public health strategies. In this work, we propose and analyze a spatiotemporal epidemic model with a Holling type-II saturated incidence rate and time delay in which we incorporate two measures: vaccination and hospitalization of severe cases, as an extension of the model presented by Diagne et al. [14]. The Holling type-II functional response is used here to capture the saturation effect observed in disease transmission [18]. In real-world scenarios, as susceptible individuals increase, contact and transmission rates do not scale linearly due to factors such as healthcare capacity limits and behavioral changes in response to rising case numbers. The Holling type-II incidence rate, therefore, provides a more accurate description of COVID-19 transmission, particularly under conditions of high incidence where linear models fail to capture this saturation effect. We formulate the optimal control problem as a system of delayed reaction-diffusion equations. We verify that this problem is mathematically and biologically well-posed, then we demonstrate that the system has a unique strong solution, and we characterize the optimal controls. We conclude our work by presenting numerical simulations for different scenarios to control the spread of COVID-19.

2. Mathematical model

Herein, we first present the mathematical model that describes the dynamics of the infectious disease. The population is distributed as follows: susceptible, vaccinated, infected with no severe symptoms, severe cases that required hospitalization, and recovered individuals. We assume that the initial population is in a bounded region Ω in $\mathbb{R}^2$ with a smooth boundary $\partial\Omega$ and that the habitat is spatially heterogeneous. Furthermore, we suppose that the populations in every compartment diffuse respectively with coefficients d_1, d_2, d_3, d_4 and d_5. In each position $x = (x_1, x_2)$, the number of newly infected per time unit is proportional to $\frac{SI(x,t-\zeta)}{1+\alpha I(x,t-\zeta)} + \delta\frac{VI(x,t-\zeta)}{1+\alpha I(x,t-\zeta)}$ where ζ is the latent period and $1-\delta$ is the vaccine efficacy. The incidence terms $\frac{\beta SI(x,t-\zeta)}{1+\alpha I(x,t-\zeta)}$ and $\delta\frac{\beta VI(x,t-\zeta)}{1+\alpha I(x,t-\zeta)}$ describe the Holling type II incidence rates associated respectively to susceptible and vaccinated subpopulations where β is the transmission rate. Both incidence terms include a time-delayed factor $(t-\zeta)$ to realistically model transmission rates based on infectiousness onset. By incorporating a delay in the incidence, the model effectively captures the staggered nature of COVID-19 transmission, where infections in various spatial locations reflect not only current cases but also cases arising from earlier periods due to latent infections. Additionally, the model accounts for the dynamics of immunity loss through the term λR,

which signifies the gradual waning of immunity over time. This aligns with the biological reality that individuals who recover from infection may lose their protective immunity, leading to a transition back into the susceptible compartment at a rate proportional to λ. Clinical trials for COVID-19 vaccines initially reported high efficacy rates shortly after completing the vaccination regimen [29]. However, subsequent studies revealed a gradual decline in antibody levels and neutralization capacity against emerging variants over time, with significant waning observed around the three-month mark [39, 43]. This decline results from a reduced ability to respond to future infections, compounded by decreasing antibody levels. While the presence of antibodies is an important indicator of immunity, the immune system also relies on memory B cells and T cells for long-term protection. λ quantifies the rate of immunity loss, ensuring that the model accurately captures the epidemiological implications of waning immunity on the dynamics of disease spread and control.

Using the above assumptions we propose our model with Neumann boundary condition:

$$\begin{cases} \partial_t S(x,t) = d_1 \Delta S + \Pi - \frac{\beta S I(x,t-\zeta)}{1+\alpha I(x,t-\zeta)} + \lambda R - (v+\mu) S, \\ \partial_t V(x,t) = d_2 \Delta V + vS - \delta \frac{\beta V I(x,t-\zeta)}{1+\alpha I(x,t-\zeta)} - \mu V, \\ \partial_t I(x,t) = d_3 \Delta I + \frac{\beta S I(x,t-\zeta)}{1+\alpha I(x,t-\zeta)} + \delta \frac{\beta V I(x,t-\zeta)}{1+\alpha I(x,t-\zeta)} - (r+\mu)\, I, \\ \partial_t I_s(x,t) = d_4 \Delta I_s + r(1-\xi) I - (\gamma + d + \mu)\, I_s, \\ \partial_t R(x,t) = d_5 \Delta R + \gamma I_s + r\xi I - (\lambda + \mu)\, R. \end{cases} \tag{2.1}$$

$$\partial_\eta S = \partial_\eta V = \partial_\eta I = \partial_\eta I_s = \partial_\eta R = 0, \quad on \quad \partial\Omega \times \mathbb{R}^+. \tag{2.2}$$

where η is the outward unit normal vector on the boundary.

Let $\psi_1, \psi_2, \psi_3, \psi_4, \psi_5$ be nonnegative, bounded functions on $\Omega \times [-\zeta, 0]$ such that $\psi = (\psi_1, \psi_2, \psi_3, \psi_4, \psi_5) \in C\left([-\zeta, 0], C\left(\overline{\Omega}, \mathbb{R}^5\right)\right)$ and $\psi(\theta, .)$ is uniformly continuous for $\theta \in [-\zeta, 0]$. The initial conditions are given, for all $(x, \theta) \in \Omega \times [-\zeta, 0]$, by:

$$\begin{aligned} S(x,\theta) =& \psi_1(x,\theta),\ V(x,\theta) = \psi_2(x,\theta),\ I(x,\theta) = \psi_3(x,\theta), \\ I_s(x,\theta) =& \psi_4(x,\theta) \quad and \quad R(x,\theta) = \psi_5(x,\theta). \end{aligned} \tag{2.3}$$

3. Basic properties

Let us define:

$$\ell = (\ell_1, \ell_2, \ell_3, \ell_4, \ell_5) = (S, V, I, I_s, R).$$

If we consider the function Ψ defined by :

$$\Psi(t, \Phi) = (\Psi_1(t, \Phi),\ \Psi_2(t, \Phi),\ \Psi_3(t, \Phi),\ \Psi_4(t, \Phi),\ \Psi_5(t, \Phi)) \tag{3.1}$$

Symbols	Meaning
Π	Birth rate
α	Saturation rate
μ	Natural death rate
β	Transmission rate
γ	Recovery rate due to treatment and hospitalization
v	Vaccination rate
$1-\delta$	Vaccine efficacy
r	Rate at which individuals leave the infected compartment
$r\xi$	Rate at which the infected individuals recover without hospitalization
d	Disease induced death rate
λ	Loss of immunity rate
ζ	Latent period

Table 1. The different parameters and constants

with

$$\begin{cases} \Psi_1(t,\Phi)(x) = \Pi - \frac{\beta\Phi_1(x,0)\Phi_3(x,-\zeta)}{1+\alpha\Phi_3(x,-\zeta)} + \lambda\Phi_5(x,0) - (v+\mu)\Phi_1(x,0), \\ \Psi_2(t,\Phi)(x) = v\Phi_1(x,0) - \delta\frac{\beta\Phi_2(x,0)\Phi_3(x,-\zeta)}{1+\alpha\Phi_3(x,-\zeta)} - \mu\Phi_2(x,0), \\ \Psi_3(t,\Phi)(x) = \frac{\beta\Phi_1(x,0)\Phi_3(x,-\zeta)}{1+\alpha\Phi_3(x,-\zeta)} + \delta\frac{\beta\Phi_2(x,0)\Phi_3(x,-\zeta)}{1+\alpha\Phi_3(x,-\zeta)} - (r+\mu)\,\Phi_3(x,0), \\ \Psi_4(t,\Phi)(x) = r(1-\xi)\Phi_3(x,0) - (\gamma+d+\mu)\,\Phi_4(x,0), \\ \Psi_5(t,\Phi)(x) = r\xi\Phi_3(x,0) + \gamma\Phi_4(x,0) - (\lambda+\mu)\,\Phi_5(x,0), \end{cases} \tag{3.2}$$

and

$$\Phi = (\Phi_1, \Phi_2, \Phi_3, \Phi_4, \Phi_5),$$

then the problem (2.1)-(2.3) can be written in the form:

$$\begin{cases} \partial_t \ell(t) = A\ell(t) + \Psi(t,\ell_t)\,, \quad t>0, \\ \ell_0 = \psi, \end{cases} \tag{3.3}$$

where ℓ_t denotes the continuous function given by $\ell_t(\theta) = \ell(t+\theta)$ for $\theta \in [-\zeta, 0]$ and A is the following linear operator:

$$A = \begin{pmatrix} d_1\Delta & 0 & 0 & 0 & 0 \\ 0 & d_2\Delta & 0 & 0 & 0 \\ 0 & 0 & d_3\Delta & 0 & 0 \\ 0 & 0 & 0 & d_4\Delta & 0 \\ 0 & 0 & 0 & 0 & d_5\Delta \end{pmatrix}.$$

Since Ψ is locally Lipschitz, we deduce from [47] that the problem (2.1) - (2.3) has a unique noncontinuable solution. Moreover, by the maximum principle we can show that this solution is nonnegative and admits upper limit.

4. Stability analysis

First, we linearize the dynamical system (2.1) around arbitrary steady state $\bar{E}(\bar{S}, \bar{V}, \bar{I}, \bar{I}_s, \bar{R})$ for small space and time dependent fluctuations and expand them into Fourier space. For this, let $\ell(x,t) = e^{\rho t + i(k_{x_1}x_1 + k_{x_2}x_2)}\tilde{\ell}$, where ρ is the frequency, k_{x_1} and k_{x_2} are respectively the wave parameters in the directions x_1 and x_2 such that $x = (x_1, x_2)$, and $\bar{\ell} = (\bar{S}, \bar{V}, \bar{I}, \bar{I}_s, \bar{R})$. Substituting $\ell(x,t)$ in (2.1), we get the following characteristic equation:

$$det \begin{pmatrix} \rho + \frac{\beta\bar{I}e^{-\rho\zeta}}{1+\alpha\bar{I}e^{-\rho\zeta}} + v + \mu + k_x^2 d_1 & 0 & \frac{\beta\bar{S}e^{-\rho\zeta}}{(1+\alpha\bar{I}e^{-\rho\zeta})^2} & 0 & -\lambda \\ -v & \rho + \mu + k_x^2 d_2 & \frac{\delta\beta\bar{V}e^{-\rho\zeta}}{(1+\alpha\bar{I}e^{-\rho\zeta})^2} & 0 & 0 \\ -\frac{\beta\bar{I}e^{-\rho\zeta}}{1+\alpha\bar{I}e^{-\rho\zeta}} & -\frac{\delta\beta\bar{I}e^{-\rho\zeta}}{1+\alpha\bar{I}e^{-\rho\zeta}} & \rho - \frac{\beta(\bar{S}+\delta\bar{V})e^{-\rho\zeta}}{(1+\alpha\bar{I}e^{-\rho\zeta})^2} + r + \mu + k_x^2 d_3 & 0 & 0 \\ 0 & 0 & -r(1-\xi) & \rho + \gamma + d + \mu + k_x^2 d_4 & 0 \\ 0 & 0 & -r\xi & -\gamma & \rho + \lambda + \mu + k_x^2 d_5 \end{pmatrix} = 0 \tag{4.1}$$

with $k_x^2 = k_{x_1}^2 + k_{x_2}^2$.

4.1. Disease-free equilibrium

Using the next generation matrix method, the basic reproduction number of disease in the absence of spatial diffusion is given by: $R_0 = \frac{\beta\Pi(\mu+\delta v)}{\mu(r+\mu)(v+\mu)}$. The model always admits a disease-free equilibrium (DFE) $E_0 = (S_0, V_0, 0, 0, 0) = (\frac{\Pi}{v+\mu}, \frac{v\Pi}{\mu(v+\mu)}, 0, 0, 0)$ which is feasible. The characteristic equation associated to system (2.1) and evaluated at E_0 is given by:

$$\begin{aligned} &\left(\rho + v + \mu + k_x^2 d_1\right)\left(\rho + \mu + k_x^2 d_2\right)\left(\rho + r + \mu + k_x^2 d_3 - \frac{\beta\Pi(\mu+\delta v)}{\mu(v+\mu)}e^{-\rho\zeta}\right), \\ &\left(\rho + \gamma + d + \mu + k_x^2 d_4\right)\left(\rho + \lambda + \mu + k_x^2 d_5\right) = 0. \end{aligned}$$

The solutions $\rho_1(k_x) = -(v+\mu) - k_x^2 d_1$, $\rho_2(k_x) = -\mu - k_x^2 d_2$, $\rho_3(k_x) = -(\gamma + d + \mu) - k_x^2 d_4$ and $\rho_4(k_x) = -(\lambda + \mu) - k_x^2 d_5$ are negative. Let us define $R_m(k_x) = \frac{\beta\Pi(\mu+\delta v)}{\mu(r+\mu+k_x^2 d_3)(v+\mu)} = \frac{r+\mu}{r+\mu+k_x^2 d_3}R_0$. Assume that $R_0 < 1$ (which implies that $R_m(k_x) <$

0) and let us suppose that the equation $\rho + r + \mu + k_x^2 d_3 - \frac{\beta\Pi(\mu+\delta v)}{\mu(v+\mu)} e^{-\rho\zeta} = 0$ admits a solution $\rho_5(k_x)$ such that $Re(\rho_5(k_x)) \geq 0$. Then $Re(\rho_5(k_x)) \leq \frac{\beta\Pi(\mu+\delta v)}{\mu(v+\mu)} - k_x^2 d_3 - r - \mu = (r+\mu)(R_m(k_x) - 1) < 0$. We obtain a contradiction which implies that: $Re(\rho_5(k_x)) < 0$ for all k_x. Hence E_0 is asymptotically stable. If $R_0 > 1$ then, by using the intermediate value theorem, we can show that the equation $\rho + r + \mu + k_x^2 d_3 - \frac{\beta\Pi(\mu+\delta v)}{\mu(v+\mu)} e^{-\rho\zeta} = 0$ has a positive real root if $k_x = 0$. Hence E_0 is unstable.

Let us now analyze the stability behavior of E_0 at $R_0 = 1$. The characteristic equation associated to (2.1) and evaluated at $R_0 = 1$ and $\beta = \frac{\mu(r+\mu)(v+\mu)}{\Pi(\mu+\delta v)} = \beta^*$:

$$det \begin{pmatrix} \rho+v+\mu+k_x^2 d_1 & 0 & -\frac{\beta^*\Pi}{v+\mu}e^{-\rho\zeta} & 0 & -\lambda \\ -v & \rho+\mu+k_x^2 d_2 & -\frac{\beta^*\delta v\Pi}{\mu(v+\mu)}e^{-\rho\zeta} & 0 & 0 \\ 0 & 0 & \rho+k_x^2 d_3 & 0 & 0 \\ 0 & 0 & -r(1-\xi) & \rho+\gamma+d+\mu+k_x^2 d_4 & 0 \\ 0 & 0 & -r\xi & -\gamma & \rho+\lambda+\mu+k_x^2 d_5 \end{pmatrix} = 0$$

has five negative roots. Hence, we proved the following result:

Theorem 4.1. *If $R_0 \leq 1$ then the DFE E_0 is asymptotically stable, and it is unstable if $R_0 > 1$.*

4.2. Endemic equilibrium

Let us determine under what conditions does the system (2.1) admits an endemic equilibrium $E_1(S^e, V^e, I^e, I_s^e, R^e)$. We make the right side of the system (2.1) equal to 0 which is rearranged to obtain:

$$\begin{aligned} S^e &= \left(\Pi + \tfrac{\lambda(r\xi(d+\mu)+\gamma r)I^e}{(\lambda+\mu)(\gamma+d+\mu)}\right)/\left(\tfrac{\beta I^e}{1+\alpha I^e}+v+\mu\right), \\ V^e &= (r+\mu)/\left(\tfrac{\beta}{\mu}(\mu+\tfrac{\delta\beta I^e}{1+\alpha I^e})+\tfrac{\delta\beta}{1+\alpha I^e}\right), \\ I_s^e &= \tfrac{r(1-\xi)I^e}{(\gamma+d+\mu)}, \\ R^e &= \tfrac{r\xi(d+\mu)+\gamma r}{(\lambda+\mu)(\gamma+d+\mu)} I^e. \end{aligned}$$

I^e is given by the quadratic equation:

$$A_2 I^{e2} + A_1 I^e + A_0 = 0, \tag{4.2}$$

where

$$\begin{aligned} A_2 =& \left(\frac{\lambda\gamma r(1-\xi)}{(\lambda+\mu)(\gamma+d+\mu)} + \frac{\lambda r\xi}{\lambda+\mu} - (r+\mu)\right)(\mu\alpha+\delta\beta) < 0, \\ A_1 =& \Pi(\mu\alpha+\delta\beta) + (\mu+\delta\beta)\left(\frac{\lambda\gamma r(1-\xi)}{(\lambda+\mu)(\gamma+d+\mu)} + \frac{\lambda r\xi}{\lambda+\mu} - (r+\mu)\right) \\ & - \frac{\mu^2(r+\mu)}{v\beta}\left(\alpha(v+\mu)+\delta\beta\right), \\ A_0 =& \Pi\left(\mu+\delta\beta\right) - \frac{\mu^2(r+\mu)}{v\beta}\left(v+\mu+\delta\beta\right). \end{aligned}$$

By using Descartes' rule of signs, the equation (4.2) admits a unique positive real solution I^e (which means that the system (2.1) admits a unique endemic equilibrium) if any one of the following conditions is verified:

- $A_1 > 0$ and $A_0 > 0$,
- $A_1 < 0$ and $A_0 > 0$.

Theorem 4.2. *The system* (2.1) *admits a unique endemic equilibrium* E_1 *if* $A_1 \neq 0$ *and* $A_0 > 0$.

The characteristic equation of system (2.1) evaluated at the endemic equilibrium E_1 is given by:

$$\rho^5 + B_4\rho^4 + B_3\rho^3 + B_2\rho^2 + B_1\rho + B_0 + \left(C_4\rho^4 + C_3\rho^3 + C_2\rho^2 + C_1\rho + C_0\right)e^{-\rho\zeta} = 0 \tag{4.3}$$

where

$$\begin{aligned}
B_4 =& r + u + \gamma + d + \lambda + 5\mu + \frac{(\delta+1)\beta I^e}{1+\alpha I^e},\\
B_3 =& \left(\mu + \frac{\delta\beta I^e}{1+\alpha I^e}\right)(r+\mu) + (\gamma + d + \mu)(\lambda + \mu)\\
&+ \left(\frac{\beta I^e}{1+\alpha I^e} + u + \gamma + d + \lambda + 3\mu\right)\left(\frac{\delta\beta I^e}{1+\alpha I^e} + r + 2\mu\right)\\
&+ \left(\frac{\beta I^e}{1+\alpha I^e} + u + \mu\right)(\gamma + d + \lambda + 2\mu),\\
B_2 =& \left(\frac{\beta I^e}{1+\alpha I^e} + u + \mu\right)(\gamma + d + \mu)(\lambda + \mu) - \lambda r\xi\frac{\beta I^e}{1+\alpha I^e}\\
&+ \left(\frac{\beta I^e}{1+\alpha I^e} + u + \gamma + d + \lambda + 3\mu\right)\left(\mu + \frac{\delta\beta I^e}{1+\alpha I^e}\right)(r+\mu)\\
&+ \left[(\gamma + d + \mu)(\lambda + \mu) + \left(\frac{\beta I^e}{1+\alpha I^e} + u + \mu\right)(\gamma + d + \lambda + 2\mu)\right]\\
&\left(\frac{\delta\beta I^e}{1+\alpha I^e} + r + 2\mu\right),\\
B_1 =& \left(\frac{\delta\beta I^e}{1+\alpha I^e} + r + 2\mu\right)\left(\frac{\beta I^e}{1+\alpha I^e} + u + \mu\right)(\gamma + d + \mu)(\lambda + \mu)\\
&- \frac{\lambda r\beta I^e}{1+\alpha I^e}\left[(\xi(d+\mu) + \gamma) + \xi\left(\mu + \delta u + \frac{\delta\beta I^e}{1+\alpha I^e}\right)\right]\\
&+ \left[(\gamma + d + \mu)(\lambda + \mu) + \left(\frac{\beta I^e}{1+\alpha I^e} + u + \mu\right)(\gamma + d + \lambda + 2\mu)\right]\\
&\left(\mu + \frac{\delta\beta I^e}{1+\alpha I^e}\right)(r+\mu),\\
B_0 =& \left(\frac{\beta I^e}{1+\alpha I^e} + u + \mu\right)(\gamma + d + \mu)(\lambda + \mu)\left(\mu + \frac{\delta\beta I^e}{1+\alpha I^e}\right)(r+\mu)\\
&- (\lambda r\xi(d+\mu) + \lambda r\gamma)\frac{\beta I^e}{1+\alpha I^e}\left(\mu + \delta u + \frac{\delta\beta I^e}{1+\alpha I^e}\right)
\end{aligned}$$

$$+\frac{\beta S^e}{1+\alpha I^e}\left[(\gamma+d+\lambda+2\mu)\left(\left(\mu+\frac{\delta\beta I^e}{1+\alpha I^e}\right)\frac{\beta I^e}{1+\alpha I^e}+\frac{\delta u\beta I^e}{1+\alpha I^e}\right)\right.$$
$$\left.+\frac{\beta I^e}{1+\alpha I^e}(\gamma+d+\mu)(\lambda+\mu)\right].$$

$$C_4=-\frac{\beta S^e+\delta\beta V^e}{(1+\alpha I^e)^2},$$
$$C_3=-\frac{\beta S^e+\delta\beta V^e}{(1+\alpha I^e)^2}\left(\frac{(\delta+1)\beta I^e}{1+\alpha I^e}+u+\gamma+d+\lambda+4\mu\right)+\frac{\delta^2\beta^2 I^e V^e}{(1+\alpha I^e)^3},$$
$$C_2=-\frac{\beta S^e+\delta\beta V^e}{(1+\alpha I^e)^2}\left(\frac{\beta I^e}{1+\alpha I^e}+u+\gamma+d+\lambda+3\mu\right)\left(\mu+\frac{\delta\beta I^e}{1+\alpha I^e}\right)$$
$$-\frac{\beta S^e+\delta\beta V^e}{(1+\alpha I^e)^2}\left[(\gamma+d+\mu)(\lambda+\mu)+\left(\frac{\beta I^e}{1+\alpha I^e}+u+\mu\right)(\gamma+d+\lambda+2\mu)\right]$$
$$+\frac{\delta^2\beta^2 I^e V^e}{(1+\alpha I^e)^3}\left(\frac{\beta I^e}{1+\alpha I^e}+u+\gamma+d+\lambda+3\mu\right)+(\gamma+d+\lambda+2\mu)\frac{\beta I^e}{1+\alpha I^e}$$
$$+\frac{\beta S^e}{1+\alpha I^e}\left[\frac{\delta u\beta I^e}{1+\alpha I^e}+\left(\mu+\frac{\delta\beta I^e}{1+\alpha I^e}\right)\frac{\beta I^e}{1+\alpha I^e}\right],$$
$$C_1=\left[(\gamma+d+\mu)(\lambda+\mu)+\left(\frac{\beta I^e}{1+\alpha I^e}+u+\mu\right)(\gamma+d+\lambda+2\mu)\right]\left[\frac{\delta^2\beta^2 I^e V^e}{(1+\alpha I^e)^3}\right.$$
$$\left.-\left(\mu+\frac{\delta\beta I^e}{1+\alpha I^e}\right)\frac{\beta S^e+\delta\beta V^e}{(1+\alpha I^e)^2}\right]-\frac{\beta S^e+\delta\beta V^e}{(1+\alpha I^e)^2}\left(\frac{\beta I^e}{1+\alpha I^e}+u+\mu\right)(\gamma+d+\mu)$$
$$+\frac{\beta S^e}{1+\alpha I^e}\left[(\gamma+d+\lambda+2\mu)\left(\left(\mu+\frac{\delta\beta I^e}{1+\alpha I^e}\right)\frac{\beta I^e}{1+\alpha I^e}+\frac{\delta u\beta I^e}{1+\alpha I^e}\right)\right.$$
$$\left.+\frac{\beta I^e}{1+\alpha I^e}(\gamma+d+\mu)(\lambda+\mu)\right],$$
$$C_0=\frac{\beta S^e}{1+\alpha I^e}\left[\left(\mu+\frac{\delta\beta I^e}{1+\alpha I^e}\right)\frac{\beta I^e}{1+\alpha I^e}+\frac{\delta u\beta I^e}{1+\alpha I^e}\right]$$
$$+\left(\frac{\beta I^e}{1+\alpha I^e}+u+\mu\right)(\gamma+d+\mu)(\lambda+\mu)\left[\frac{\delta^2\beta^2 I^e V^e}{(1+\alpha I^e)^3}\right.$$
$$\left.-\left(\mu+\frac{\delta\beta I^e}{1+\alpha I^e}\right)\frac{\beta S^e+\delta\beta V^e}{(1+\alpha I^e)^2}\right].$$

Let us define: $B_0^{'}=B_0+C_0$, $B_1^{'}=B_1+C_1$, $B_2^{'}=B_2+C_2$, $B_3^{'}=B_3+C_3$, and $B_4^{'}=B_4+C_4$.

Theorem 4.3. *The endemic equilibrium E_1 is locally asymptotically stable for $\zeta=0$ if $B_4^{'}>0$, $B_4^{'}B_3^{'}-B_2^{'}>0$, $(B_1^{'}B_2^{'}-B_0^{'}B_3^{'})/B_2^{'}>0$, and $(B_4^{'}B_3^{'}-B_2^{'})B_2^{'}/B_4^{'}-(B_1^{'}B_2^{'}-B_0^{'}B_3^{'})B_4^{'}/B_2^{'}>0$.*

Proof. If $\zeta=0$, then the equation (4.3) reduces to:

$$\rho^5+B_4^{'}\rho^4+B_3^{'}\rho^3+B_2^{'}\rho^2+B_1^{'}\rho+B_0^{'}=0$$

and by using the Routh–Hurwitz criterion, we get the result. □

Once again, we need to define: $D_4 = B_4^2 - 2B_3 - C_4^2$, $D_3 = B_3^2 + 2B_1 - 2B_2B_4 - C_3^2 + 2C_2C_4$, $D_2 = B_2^2 + 2B_0B_4 - 2B_1B_3 - 2C_0C_4 + 2C_1C_3 - C_2^2$, $D_1 = B_1^2 - 2B_0B_2 - C_1^2 + 2C_0C_2$ and $D_0 = B_0^2 - C_0^2$.

Theorem 4.4. *The endemic equilibrium E_1 is locally asymptotically stable for $\zeta > 0$ if $D_4 > 0$, $D_4D_3 - D_2 > 0$, $(D_1D_2 - D_0D_3)/D_2 > 0$, and $(D_4D_3 - D_2)D_2/D_4 - (D_1D_2 - D_0D_3)D_4/D_2 > 0$.*

Proof. If the endemic equilibrium E_1 is unstable for a value of ζ it follows that, from [34], there exists $\theta > 0$ such that $\rho = i\theta$ is a root of the characteristic equation (4.3). By contradiction, suppose such a root exists. It follows that:

$$\left(C_3\theta^3 - C_1\theta\right) cos(\theta\zeta) + \left(C_4\theta^4 - C_2\theta^2 + C_0\right) sin(\theta\zeta) = \theta^5 - B_3\theta^3 + B_1\theta, \tag{4.4}$$

$$\left(C_4\theta^4 - C_2\theta^2 + C_0\right) cos(\theta\zeta) - \left(C_3\theta^3 - C_1\theta\right) sin(\theta\zeta) = -B_4\theta^4 + B_2\theta^2 - B_0, \tag{4.5}$$

which implies:

$$\left(\left(C_3\theta^3 - C_1\theta\right) cos(\theta\zeta) + \left(C_4\theta^4 - C_2\theta^2 + C_0\right) sin(\theta\zeta)\right)^2 = \left(\theta^5 - B_3\theta^3 + B_1\theta\right)^2, \tag{4.6}$$

$$\left(\left(C_4\theta^4 - C_2\theta^2 + C_0\right) cos(\theta\zeta) - \left(C_3\theta^3 - C_1\theta\right) sin(\theta\zeta)\right)^2 = \left(B_4\theta^4 - B_2\theta^2 + B_0\right)^2. \tag{4.7}$$

By adding both sides of (4.6) and (4.7), we get:

$$\theta^{10} + D_4\theta^8 + D_3\theta^6 + D_2\theta^4 + D_1\theta^2 + D_0 = 0. \tag{4.8}$$

Let $X = \theta^2$,the equation (4.8) becomes:

$$X^5 + D_4X^4 + D_3X^3 + D_2X^2 + D_1X + D_0 = 0. \tag{4.9}$$

According to the Routh–Hurwitz criterion, because all the roots of the equation (4.9) have negative real parts if the theorem's conditions are met, we get a contradiction, and thus the endemic equilibrium E_1 is locally asymptotically stable for all $\zeta > 0$. □

5. Optimal control problem

The two controls in this section, v and γ, are functions of time and space. The vaccination strategy implemented focuses on immunizing a sufficient number of individuals based on their spatial location to effectively eradicate the epidemic. By considering the spatial distribution of the population, the strategy optimizes vaccination efforts to target areas with the highest concentration of susceptible and infected individuals. This spatially adaptive approach aims to minimize the density of susceptible individuals, infected individuals, and severe cases while minimizing the cost of vaccination and hospitalization by focusing resources where they're most needed, minimizing wasted efforts and costs. We obtain the following control problem:

$$\begin{cases} \partial_t S = d_1 \Delta S + \Pi - \frac{\beta S(x,t) I(x,t-\zeta)}{1+\alpha I(x,t-\zeta)} + \lambda R(x,t) - (v(x,t)+\mu) S(x,t), \\ \partial_t V = d_2 \Delta V + v(x,t) S(x,t) - \delta \frac{\beta V(x,t) I(x,t-\zeta)}{1+\alpha I(x,t-\zeta)} - \mu V(x,t), \\ \partial_t I = d_3 \Delta I + \frac{\beta S(x,t) I(x,t-\zeta)}{1+\alpha I(x,t-\zeta)} + \delta \frac{\beta V(x,t) I(x,t-\zeta)}{1+\alpha I(x,t-\zeta)} - (r+\mu) I(x,t), \ (x,t) \in \Xi, \\ \partial_t I_s = d_4 \Delta I_s + r(1-\xi) I(x,t) - (\gamma(x,t) + d + \mu) I_s(x,t), \\ \partial_t R = d_5 \Delta R + r\xi I(x,t) + \gamma(x,t) I_s(x,t) - (\lambda + \mu) R(x,t). \end{cases} \tag{5.1}$$

with Neumann conditions:

$$\partial_\eta S = \partial_\eta V = \partial_\eta I = \partial_\eta I_s = \partial_\eta R = 0, \quad on \ \partial\Omega \times [0,T], \tag{5.2}$$

$$S = \psi_1, \ V = \psi_2, \ I = \psi_3, \ I_s = \psi_4 \ and \ R = \psi_5 \ on \ \Omega \times [-\zeta, 0], \tag{5.3}$$

where T represents the final time and $\Xi = \Omega \times [0,T]$. The objective functional can be given by :

$$\begin{aligned} J(S,I,R,u) = \int_0^T \int_\Omega (\kappa_1 S(x,t) + \kappa_2 I(x,t) + \kappa_3 I_s(x,t)) \, dxdt \\ + \frac{\alpha_1}{2} \|v\|^2_{L^2(\Xi)} + \frac{\alpha_2}{2} \|\gamma\|^2_{L^2(\Xi)}, \end{aligned} \tag{5.4}$$

where $(v,\gamma) \in U_{ad} = \{(v,\gamma) \in L^\infty(\Xi); \ 0 \le v \le v_{max} \ and \ 0 \le \gamma \le \gamma_{max} \ on \ \Xi\}$.

The constants κ_1, κ_2, κ_3, α_1 and α_2 are balancing constants related to cost factors. Since there is no linear relationship between the effects of intervention and the cost of intervention (the total cost includes the cost of treatment, beds, transport,...), we use a nonlinear cost functional. In this sequel, we apply the quadratic objective functional for measuring the cost of the control as used in several works [1, 33, 45, 46].

The control variables v and γ interact with the state variables in the following ways:

- Vaccination Impact: The vaccination rate $v(x,t)$ affects the susceptible population S directly, as it increases the number of vaccinated individuals V while simultaneously decreasing the number of susceptible individuals. The term $v(x,t)S(x,t)$ in the equation for $\partial_t V$ captures this interaction, as it indicates that the vaccination of susceptible individuals is proportional to their current population density.
- Hospitalization Dynamics: The hospitalization rate $\gamma(x,t)$ interacts with the severe cases I_s through the equation for $\partial_t I_s$. Specifically, $\gamma(x,t)$ represents the rate at which severe cases transition out of the infected compartment into the recovered state, thereby impacting the dynamics of both the I_s and R populations. The term $\gamma(x,t)I_s(x,t)$ indicates that the effectiveness of hospitalization in reducing the severity of the outbreak is influenced by the current number of severe cases.

6. Existence of global solution

In order to reformulate the model (5.1)-(5.3), let:

$$\mathcal{H} = \left(L^2(\Omega)\right)^5,$$

$$\ell = (\ell_1, \ell_2, \ell_3, \ell_4, \ell_5) = (S, V, I, I_s, R),$$

and let us consider the following linear operator:

$$\mathcal{A} : D(\mathcal{A}) \subset \mathcal{H} \to \mathcal{H},$$

$$\mathcal{A} = \begin{pmatrix} d_1\Delta & 0 & 0 & 0 & 0 \\ 0 & d_2\Delta & 0 & 0 & 0 \\ 0 & 0 & d_3\Delta & 0 & 0 \\ 0 & 0 & 0 & d_4\Delta & 0 \\ 0 & 0 & 0 & 0 & d_5\Delta \end{pmatrix},$$

where

$$D(\mathcal{A}) = \left\{ \ell \in \left(H^2(\Omega)\right)^5, \frac{\partial \ell_1}{\partial \eta} = \frac{\partial \ell_2}{\partial \eta} = \frac{\partial \ell_3}{\partial \eta} = \frac{\partial \ell_4}{\partial \eta} = \frac{\partial \ell_5}{\partial \eta} = 0, \ a.e\ x \in \partial\Omega \right\}. \quad (6.1)$$

The controlled system can be rewritten in the form:

$$\begin{cases} \partial_t \ell = \mathcal{A}\ell(t) + \Psi(t, \ell_t)\ , \quad t \in [0, T], \\ \ell_0 = \psi. \end{cases} \quad (6.2)$$

Lemma 6.1. *Let X be a Banach space, $(T(t))_{t\geq 0}$ a strongly continuous semigroup of bounded linear operators on X satisfying $\|T(t)\| \leq Me^{\omega t}$ for all $t \geq 0$ (M and ω are fixed constants) and let $\psi \in C([-\zeta, 0]; X)$ be a given function. If a function $\Psi : [0, T] \times C([-\zeta, 0]; X)$ is measurable in the first variable and satisfies the following conditions:*

i. A Lipschitz condition:

$$\|\Psi(t, \varphi) - \Psi(t, \tilde{\varphi})\| \leq L \|\varphi - \tilde{\varphi}\|\ , \quad t \in [0, T],\ \varphi, \tilde{\varphi} \in C([-\zeta, 0]; X).$$

ii. $\Psi(., 0) \in L^1([0, T], X)$;

iii. There exists a constant K such that: $\|\Psi(t, \psi)\| \leq K$ for all $t \in [0, T]$.

then the initial value problem of abstract integral equation given by:

$$\begin{cases} \ell(t) = T(t)\psi(0) + \int_0^t T(t-s)\Psi(s, \ell_s)ds \\ \ell_0 = \psi \end{cases}, \ t \in [0, T] \quad (6.3)$$

admits a unique solution $\ell : [-\zeta, T] \to X$.

Proof. From conditions (i) and (ii), we can see that $\Psi(t,\varphi) \in L^1([0,T],X)$ for all $\varphi \in C([-\zeta,0];X)$. Let us define:

$$\ell^0(t) = \begin{cases} \psi(t) & , \ t \in [-\zeta,0], \\ T(t)\psi(0) & , \ t \in [0,T], \end{cases}$$

and for each positive integer n:

$$\ell^n(t) = \begin{cases} \psi(t) & , \ t \in [-\zeta,0], \\ T(t)\psi(0) + \int_0^t T(t-s)\Psi(s,\ell_s^{n-1})ds & , \ t \in [0,T]. \end{cases}$$

By using condition (iii), we can show that there exists a constant K' such that $\|\Psi(s,\ell_s^0)\| \leq K'$ for all $s \in [0,T]$. Then for $0 \leq t \leq T$,

$$\|\ell^1(t) - \ell^0(t)\| \leq K' e^{\omega T} t$$

and, by recurrence,

$$\|\ell^n(t) - \ell^{n-1}(t)\| \leq K' L^{n-1} e^{n\omega T} \frac{t^n}{n!}.$$

Hence, the limit $\ell(t) = \lim_{n\to\infty} \ell^n(t)$ converges uniformly on $[-\zeta,T]$.

To verify that $\ell(t)$ satisfies (6.3), notice that:

$$\begin{aligned} &\|\ell(t) - T(t)\psi(0) - \int_0^t T(t-s)\Psi(s,\ell_s)ds\| \\ &\leq \|\ell(t) - \ell^{n+1}(t)\| + \| \int_0^t T(t-s)\left[\Psi(s,\ell_s) - \Psi(s,\ell_s^n)\right] ds\| \\ &\leq \|\ell(t) - \ell^{n+1}(t)\| + Le^{\omega T} \int_0^t \|\ell_s - \ell_s^n\| ds. \end{aligned}$$

Moreover,

$$\ell(t) - \ell^n(t) = \sum_{k=n+1}^{\infty} \left(\ell^k(t) - \ell^{k-1}(t)\right).$$

It follows that:

$$\|\ell(t) - T(t)\psi(0) - \int_0^t T(t-s)\Psi(s,\ell_s)ds\| \leq \left[1 + Le^{\omega T} t\right] K' \sum_{k=n+1}^{\infty} L^{k-1} e^{k\omega T} \frac{t^k}{k!},$$

and consequently we obtain $\ell(t) = T(t)\psi(0) + \int_0^t T(t-s)\Psi(s,\ell_s)ds$ for all $t \in [0,T]$.

We now prove uniqueness of the solution. Suppose that $\varrho(t)$ satisfies (6.3). We can find a constant K'' such that $\|\varrho(t) - \ell^1(t)\| \leq K'' t$ for all $t \in [0,T]$. Then:

$$\|\varrho(t) - \ell^n(t)\| \leq K'' L^{n-1} e^{(n-1)\omega T} \frac{t^n}{n!}.$$

Hence $\varrho(t) = \lim_{n\to\infty} \ell^n(t)$ and we deduce that $\varrho = \ell$. □

Remark 6.1. ℓ is called a mild solution of (6.2) (see [12]).

Given that our model describes the dynamics of populations subject to spatial diffusion and temporal evolution, strong solutions are crucial for ensuring that the state variables remain well-defined and behave realistically throughout the simulation. This is particularly important in epidemiological models, where continuity and differentiability can be linked to biological processes, such as the spread of infection or the response to vaccination. The strong solutions satisfy the differential equations pointwise and possess sufficient regularity (e.g., continuity and differentiability) required for the analysis of the system. This implies that the state variables not only exist but also exhibit smooth behavior over time and space. To demonstrate that (5.1)-(5.3) admits a strong solution, we need the following result (Proposition 1.1, p.174, [8])

Lemma 6.2. *Let X be a Banach space, $A : D(A) \subset X \to X$ be the infinitesimal generator of a C_0-semigroup and a function $g : [0,T] \to X$.*

- *If $z_0 \in X$ and $g \in L^1([0,T], X)$, then the problem*

$$\begin{cases} \partial_t \varrho = A\varrho(t) + g(t) \\ \varrho(0) = \varrho_0 \end{cases}, t \in [0,T]$$

  admits a unique mild solution ϱ.

- *If X is a real Hilbert space, $g \in L^2([0,T], X)$, A is self – adjoint and dissipative on X, and $\varrho_0 \in D(A)$, then the mild solution ϱ is a strong solution and $\varrho \in W^{1,2}(0,T;X) \cap L^2(0,T;D(A))$.*

The existence of a strong solution ensures that the formulated model can produce meaningful results. Without established existence, the mathematical model may not accurately reflect the dynamics of the epidemic, rendering any conclusions or insights derived from it questionable. Moreover, proving the existence of solutions confirms that the model can adequately represent the underlying biological processes governing the epidemic spread, thus validating the utility of the model in practical applications. Furthermore, the uniqueness guarantees that the model's behavior is consistent and reproducible. In other words, for given initial conditions and parameters, there will be a single trajectory of the system over time.

Theorem 6.1. *If $0 \leq \xi \leq 1$ and all the other constants in the system (5.1) are positive and ψ is a given nonnegative bounded function on $\Omega \times [-\zeta, 0]$ such that $\psi \in C([-\zeta,0];\mathcal{H})$ and $\psi(0) \in D(A)$ then, for every $(v,\gamma) \in U_{ad}$, the problem (12) − (14) admits a unique strong solution ℓ satisfying: $\ell \in W^{1,2}(0,T;\mathcal{H})$, $\ell_i \in L^2(0,T;H^2(\Omega)) \cap L^\infty(0,T;H^1(\Omega)) \cap L^\infty(\Xi)$ and $\ell_i \geq 0$ on Ξ for $i = 1,2,3,4,5$. In addition:*

$$\exists C > 0, \forall t \in [0,T], \|\partial_t \ell_i\|_{L^2(\Xi)} + \|\ell_i\|_{L^2(0,T;H^2(\Omega))} + \|\ell_i\|_{H^1(\Omega)} + \|\ell_i\|_{L^\infty(\Xi)} \leq C. \tag{6.4}$$

Proof. Since the function $\Psi(t,\varphi)$ defined in (3.1) is not Lipschitz continuous in φ uniformly in respect to $t \in [0,T]$, we can't use directly *Lemma* 6.1 to prove that the problem (4.9)-(5.2) admits a mild solution. Therefore, we need to use a truncation

procedure to $\Psi(t,\varphi)$. Let us define, for a function $h(x,t)$ and a positive integer N:

$$\begin{cases} D_h^1 = \{(x,t) : -N \leq h(x,t) \leq N\} \\ D_h^2 = \{(x,t) : h(x,t) > N\} \\ D_h^3 = \{(x,t) : h(x,t) < -N\} \end{cases} \quad and \quad h^N(x,t) = \begin{cases} h(x,t) & , (x,t) \in D_h^1 \\ N & , (x,t) \in D_h^2 \\ -N & , (x,t) \in D_h^3 \end{cases}$$

The truncation form of $\Psi(t,\ell_t)$ is defined by:

$$\Psi^N(t,\ell_t^N) = (\Psi_1^N(t,\ell_t^N),\ \Psi_2^N(t,\ell_t^N),\ \Psi_3^N(t,\ell_t^N),\ \Psi_4^N(t,\ell_t^N),\ \Psi_5^N(t,\ell_t^N))$$

is Lipschitz continuous in ℓ_t^N uniformly in respect to $t \in [0,T]$. With Lemma 6.1, it follows that:

$$\begin{cases} \partial_t \ell^N = A\ell^N(t) + \Psi^N(t,\ell_t^N) \\ \ell_0^N = \psi \end{cases}, t \in [0,T] \tag{6.5}$$

has a unique mild solution ℓ^N.

Define $g(t) = \Psi^N(t,\ell_t^N)$ for $t \in [0,T]$. Clearly, ℓ^N equals the mild solution of :

$$\begin{cases} \partial_t \varrho = A\varrho(t) + g(t) \\ \varrho(0) = \psi(0) \end{cases}, t \in [0,T].$$

Since $\Psi^N(t,\varphi) \in L^2([0,T],\mathcal{H})$ and $t \to \ell_t^N$ is continuous on $[0,T]$, we can show that $g \in L^2([0,T],\mathcal{H})$. The operator A is self-adjoint and dissipative, then, by the second part of *Lemma* 6.2, the mild solution ℓ^N is a strong solution and $\ell^N \in W^{1,2}(0,T;\mathcal{H}) \cap L^2(0,T;D(A))$. We need to verify that this strong solution is nonnegative, bounded and verifies the results of the theorem. Then we will prove that it is in fact a global solution for the problem (5.1)-(5.3).

- *STEP 1* Positivity of the solutions (i.e., non-negativity of population densities) is essential in epidemiological models, as negative populations would lack biological meaning. Proving positivity ensures that all state variables—such as susceptible, infected, and recovered individuals—remain within realistic biological bounds throughout the dynamics of the model, reinforcing the applicability of the model in real-world scenarios. We can see that $(0,0,0)$ is a lower solution of system (5.1)-(5.3). Then, we deduce that the solution ℓ^N is nonnegative.

- *STEP 2* The verification of the solutions' boundedness ensures that these solutions do not diverge to infinity, which could indicate unrealistic biological scenarios or mathematical instability. This property assures that the model remains within practical and feasible limits, allowing for meaningful interpretations of the dynamics and the effects of control measures, such as vaccination and hospitalization. To prove that $\ell^N \in (L^\infty(\Xi))^5$, we denote:

$$M_N = \max\left\{ \left\|\Psi_i^N(t,\ell_t^N)(x)\right\|_{L^\infty(\Xi)},\ \|\psi_i\|_{L^\infty([-\zeta,0]\times\Omega)}\ , i = 1,2,3,4,5 \right\}.$$

Let $\{T_i(t),\ t \geq 0\}$ be the C_0 semigroup of contractions generated by the operator B_i defined, for $i = 1,2,3,4,5$, as follows:

$B_i : D(B_i) \subset L^2(\Omega) \to L^2(\Omega)$,

$B_i\varrho = d_i\Delta\varrho$,

$D(B_i) = \left\{ \varrho \in H^2(\Omega), \frac{\partial \varrho}{\partial \eta} = 0, \text{ a.e } in\ \partial\Omega \right\}$.
The function $\tilde{\Psi}_i^N(x,t) = \ell_i^N - M_N t - \|\psi_i(.,0)\|_{L^\infty(\Omega)}$ satisfies the Cauchy problem:

$$\begin{cases} \partial_t \tilde{\Psi}_i^N(x,t) = d_i \Delta \tilde{\Psi}_i^N + \Psi_i^N(t, \ell_t^N) - M_N \\ \tilde{\Psi}_i^N(x,0) = \psi_i(x,0) - \|\psi_i(.,0)\|_{L^\infty(\Omega)} \end{cases}, t \in [0,T] \tag{6.6}$$

and the function defined by $\bar{\Psi}_i^N(x,t) = \ell_i^N + M_i^N t + \|\psi_i(.,0)\|_{L^\infty(\Omega)}$ satisfies the Cauchy problem:

$$\begin{cases} \partial_t \bar{\Psi}_i^N(x,t) = d_i \Delta \bar{\Psi}_i^N + \Psi_i^N(t, \ell_t^N) + M_N \\ \bar{\Psi}_i^N(x,0) = \psi_i(x,0) + \|\psi_i(.,0)\|_{L^\infty(\Omega)} \end{cases}, t \in [0,T], \tag{6.7}$$

then

$$\tilde{\Psi}_i^N(x,t) = T_i(t)\left(\psi_i(x,0) - \|\psi_i(.,0)\|_{L^\infty(\Omega)}\right) + \int_0^t T_i(t-s)(\Psi_i^N(s, \ell_s^N)(x) - M_N)ds$$

and

$$\bar{\Psi}_i^N(x,t) = T_i(t)\left(\psi_i(x,0) + \|\psi_i(.,0)\|_{L^\infty(\Omega)}\right) + \int_0^t T_i(t-s)(\Psi_i^N(s, \ell_s^N)(x) + M_N)ds.$$

Since we have
$\psi(x,0) - \|\psi_i(.,0)\|_{L^\infty(\Omega)} \leq 0, \quad \Psi_i^N(t, \ell_t^N)(x) - M_N \leq 0,$
$\psi_i(x,0) + \|\psi_i(.,0)\|_{L^\infty(\Omega)} \geq 0$ and $\Psi_i^N(t, \ell_t^N)(x) + M_N \geq 0$, it follows that:
$(\forall (x,t) \in \Xi)\,,\ \tilde{\Psi}_i^N(x,t) \leq 0$ and $(\forall (x,t) \in \Xi)\,,\ \bar{\Psi}_i^N(x,t) \geq 0$. Then:

$$\forall (x,t) \in \Xi,\ \|\ell_i^N(x,t)\| \leq M_N t + \|\psi_i(.,0)\|_{L^\infty(\Omega)} \tag{6.8}$$

and we conclude that, $S^N, V^N, I^N, I_s^N, R^N \in L^\infty(\Xi)$.

- *STEP 3* We now show that $S \in L^2(0,T; H^2(\Omega)) \cap L^\infty(0,T; H^1(\Omega))$. From (6.5), we get :

$$\begin{aligned} &\int_0^t \int_\Omega \left(\partial_t S^N\right)^2 ds dx + d_1^2 \int_0^t \int_\Omega \|\Delta S^N\|^2 ds dx - 2d_1 \int_0^t \int_\Omega \partial_s S^N \Delta S^N ds dx \\ &= \int_0^t \int_\Omega \left(\Pi - \tfrac{\beta S^N(x,t) I^N(x,t-\zeta)}{1+\alpha I^N(x,t-\zeta)} + \lambda R^N(x,t) - (v(x,t)+\mu) S^N(x,t)\right)^2 ds dx, \end{aligned}$$

which, by Green's formula, leads to:

$$\begin{aligned} d_1 \int_\Omega \|\nabla S^N\|^2 dx \leq &\int_0^t \int_\Omega \left(\Pi - \frac{\beta S^N I^N(x,t-\zeta)}{1+\alpha I^N(x,t-\zeta)} + \lambda R^N - (v+\mu) S^N\right)^2 ds dx \\ &+ d_1 \int_\Omega \|\nabla S^N(x,0)\|^2 dx. \end{aligned}$$

Given that $S^N(x,0) \in H^2(\Omega)$ and $S^N, I^N, R^N \in L^\infty\left([-\zeta, T] \times \Omega\right)$, then $S^N \in L^2(0,T; H^2(\Omega)) \cap L^\infty(0,T; H^1(\Omega))$. Using the same reasoning, we get V^N, I^N, I_s^N, $R^N \in L^2(0,T; H^2(\Omega)) \cap L^\infty(0,T; H^1(\Omega))$.

- *STEP 4* Let us show that the problem (5.1)-(5.3) admits a local solution. From (25), we have:

$$\forall (x,t) \in \Xi,\ \|\ell_i^N(x,t)\| \leq M_N t + \|\psi_i(.,0)\|_{L^\infty(\Omega)}.$$

By choosing N to be a positive integer such that:

$$N \geq 2\ max\left\{\|\psi_i(.,0)\|_{L^\infty(\Omega)}\ , i = 1,2,3,4,5\right\} \tag{6.9}$$

and by choosing a constant $T^{'} \in [0,T]$ such that $2T^{'}M_N \leq N$, it follows that:

$$\forall (x,t) \in \Xi^{'} = \Omega \times [0,T^{'}],\ \|\ell_i^N(x,t)\| \leq N, \tag{6.10}$$

and therefore, the problem (5.1)-(5.3) admits a local solution ℓ such that $\ell^N(x,t) = \ell(x,t)$ for all $(x,t) \in \Xi^{'}$

- *STEP 5* The local solution ℓ of $(12)-(14)$ is in fact a global solution. It suffices to prove that $S,\ V,\ I,\ I_s$ *and* R are uniformly bounded with respect to $T^{'}$.

From (12)-(14) we have:

$$\begin{cases} \partial_t S - d_1 \Delta S \leq M_1, & t \in [0,T^{'}], \\ \partial_\eta S = 0, & \\ S(x,0) = \psi_1(x,0) \leq \underset{x\in\Omega}{sup}\psi_1(x,0), & \end{cases} \tag{6.11}$$

where $M_1 = \|\Pi + \lambda R\|_{L^\infty([-\zeta,T']\times\Omega)}$. Using the comparison principle, we have for all $(x,t) \in \Xi^{'}$: $S(x,t) \leq \underset{x\in\Omega}{sup}\psi_1(x,0) + M_1 t \leq \underset{x\in\Omega}{sup}\psi_1(x,0) + M_1 T$. It follows that S is uniformly bounded with respect to $T^{'}$. Similarly, we prove that V, I, I_s *and* R are uniformly bounded with respect to $T^{'}$. Therefore ℓ is a global non-negative strong solution of (5.1)-(5.3) and $\ell \in W^{1,2}(0,T;\mathcal{H})$, $\ell_i \in L^2(0,T;H^2(\Omega)) \cap L^\infty(0,T;H^1(\Omega)) \cap L^\infty(\Xi)$, and the inequality (6.4) holds for $i = 1,2,3,4,5$. □

7. Existence of optimal solution

Let us study the existence of optimal controls that optimize the objective functional defined in (5.4).

Theorem 7.1. *The problem* (5.1)-(5.4) *has an optimal solution* (ℓ^*, v^*, γ^*) *under the same conditions as Theorem 6.3.*

Proof. Let J^* be the finite constant defined by:

$$J^* = \inf_{(v,\gamma)\in U_{ad}} \{J(\ell, v, \gamma)\}. \tag{7.1}$$

Let us consider a sequence (ℓ^n, v^n, γ^n) where:

$$v^n, \varphi^n \in U_{ad}\,,\ \ell^n \in W^{1,2}(0,T;H(\Omega))\,,\ J^* \leq J(\ell^n, v^n, \varphi^n) \leq J^* + \frac{1}{n}, \tag{7.2}$$

$$\begin{cases} \partial_t \ell_1^n = d_1 \Delta \ell_1^n + \Pi - \frac{\beta \ell_1^n(x,t)\ell_3^n(x,t-\zeta)}{1+\alpha \ell_3^n(x,t-\zeta)} + \lambda \ell_5^n(x,t) - (v^n(x,t)+\mu)\ell_1^n(x,t), \\ \partial_t \ell_2^n = d_2 \Delta \ell_2^n + v^n(x,t)\ell_1^n(x,t) - \delta \frac{\beta \ell_2^n(x,t)\ell_3^n(x,t-\zeta)}{1+\alpha \ell_3^n(x,t-\zeta)} - \mu \ell_2^n(x,t), \\ \partial_t \ell_3^n = d_3 \Delta \ell_3^n + \frac{\beta \ell_1^n(x,t)\ell_3^n(x,t-\zeta)}{1+\alpha \ell_3^n(x,t-\zeta)} + \delta \frac{\beta \ell_2^n(x,t)\ell_3^n(x,t-\zeta)}{1+\alpha \ell_3^n(x,t-\zeta)} - (r+\mu)\,\ell_3^n(x,t), \\ \partial_t \ell_4^n = d_4 \Delta \ell_4^n + r(1-\xi)\ell_3^n(x,t) - (\gamma^n(x,t)+d+\mu)\,\ell_4^n(x,t), \\ \partial_t \ell_5^n = d_5 \Delta \ell_5^n + r\xi \ell_3^n(x,t) + \gamma^n(x,t)\ell_4^n(x,t) - (\lambda+\mu)\,\ell_5^n(x,t). \end{cases} \tag{7.3}$$

$$\partial_\eta \ell_1^n = \partial_\eta \ell_2^n = \partial_\eta \ell_3^n = \partial_\eta \ell_4^n = \partial_\eta \ell_5^n = 0, \quad (x,t) \in \partial\Omega \times [0,T]. \tag{7.4}$$

$$\ell_i^n(x,\theta) = \psi_i(x,\theta) \geq 0, \tag{7.5}$$

for all $(x,\theta) \in \Omega \times [-\zeta, 0]$ and $i = 1,2,3,4,5$.

By using (6.4), (7.3) and the boundedness of ψ_1 on $\Omega \times [-\zeta, 0]$, one can find a constant K verifying:

$$\| \int_\Omega (\ell_1^n)^2(x,t)dx - \int_\Omega (\ell_1^n)^2(x,s)dx \| \leq K\|t-s\|, \tag{7.6}$$

which implies the equicontinuity at t of $\{\ell_1^n,\, n \geq 1\}$ and $\{\ell_i^n,\, n \geq 1\}$, for $i = 2,3,4,5$, similarly. Combining this with the relative compactness of $\{\ell_i^n\,, n \geq 1\}$ in $C\left([0,T]\,; L^2(\Omega)\right)$ we deduce the existence of $\ell^* \in \left(C\left([0,T]\,; L^2(\Omega)\right)\right)^5$ and a subsequence of $(\ell^n)_{n\geq 1}$ such that:

$$\begin{gathered} \ell^n \to \ell^* \; uniformly \; in \; L^2(\Omega), \\ \Delta \ell^n \to \Delta \ell^* \; weakly \; in \; L^2(\Xi), \\ \partial \ell^n \to \partial \ell_1^* \; weakly \; in \; L^2(\Xi), \\ \ell^n \to \ell^* \; weakly \; in \; L^2(0,T; H^2(\Omega)), \\ \ell^n \to \ell^* \; weakly \; in \; L^\infty(0,T; H^1(\Omega)). \end{gathered}$$

Furthermore, $\ell_1^n(x,t)\ell_3^n(x,t-\zeta) - \ell_1^*(x,t)\ell_3^*(x,t-\zeta) = \left(\ell_1^n(x,t) - \ell_1^*(x,t)\right)\ell_3^n(x,t-\zeta) + \ell_1^*(x,t)\left(\ell_3^n(x,t-\zeta) - \ell_3^*(x,t-\zeta)\right)$.

The boundedness of ℓ_1^* in $L^\infty(\Xi)$ and ℓ_3^n in $L^\infty(\Omega \times [-\zeta, T])$ combined with the convergence $\ell_1^n \to \ell_1^*$ in $L^2(\Xi)$ and the convergence $\ell_3^n \to \ell_3^*$ in $L^2(\Omega \times [-\zeta, T])$, implies:

$$\ell_1^n(x,t)\ell_3^n(x,t-\zeta) \to \ell_1^*(x,t)\ell_3^*(x,t-\zeta) \; in \; L^2(\Xi).$$

Similarly, we show that: $\ell_2^n(x,t)\ell_3^n(x,t-\zeta) \to \ell_2^*(x,t)\ell_3^*(x,t-\zeta)$ in $L^2(\Xi)$.

On the other hand, $L^2(\Xi)$ is reflexive, then there exist two subsequences v^n and γ^n for which:

$$(v^n, \gamma^n) \to (v^*, \gamma^*) \; weakly \; in \; \left(L^2(\Xi)\right)^2,$$

then $v^*, \gamma^* \in U_{ad}$ due to weak closedness of U_{ad}. Moreover:

$$\begin{gathered} v^n \ell_1^n \to v^* \ell_1^* \; in \; L^2(\Xi), \\ \gamma^n \ell_4^n \to \gamma^* \ell_4^* \; in \; L^2(\Xi). \end{gathered}$$

By applying the Aubin compactness theorem [38] and by verifying that

$$J(\ell^*, v^*, \gamma^*) \leq \inf_{u \in U_{ad}} J(\ell, v, \gamma),$$

we conclude that (ℓ^*, v^*, γ^*) is an optimal solution. □

8. First-order necessary optimality conditions

Let us start with the following lemma:

Lemma 8.1. *Suppose that all conditions of Theorem 6.3 are satisfied. For any* $(v,\gamma)\in U_{ad}$, *set* $(v^\varepsilon,\gamma^\varepsilon)=(v^*,\gamma^*)+\varepsilon(v,\gamma)\in U_{ad}$ *with* $\varepsilon>0$. *Then* (5.1)-(5.3) *has a unique strong solution* $\ell^\varepsilon=(\ell_1^\varepsilon,\ell_2^\varepsilon,\ell_3^\varepsilon,\ell_4^\varepsilon,\ell_5^\varepsilon)$ *associated to* $(v^\varepsilon,\gamma^\varepsilon)$. *Moreover,* ℓ^ε *is uniformly bounded with respect to* ε *in* Ξ.

Proof. From (5.1)-(5.3) we have:

$$\begin{cases}\partial\ell_1^\varepsilon-d_1\Delta\ell_1^\varepsilon\le M_5 \quad , \qquad t\in[0,T],\\ \partial_\eta\ell_1^\varepsilon=0,\\ \ell_1^\varepsilon(x,0)=\psi_1(x,0)\le \underset{x\in\Omega}{sup}\psi_1(x,0),\end{cases}\tag{8.1}$$

where $M_5=\|\Pi+\lambda R\|_{L^\infty(\Omega\times[-\zeta,T])}$. Using the comparison principle, we have for all $(x,t)\in\Omega\times[0,T]$: $\ell_1^\varepsilon(x,t)\le \underset{x\in\Omega}{sup}\psi_1(x,0)+M_5T$. It follows that ℓ_1^ε is uniformly bounded with respect to ε. Similarly, we can show that ℓ_2^ε, ℓ_3^ε, ℓ_4^ε and ℓ_5^ε are uniformly bounded with respect to ε. □

Let ℓ be the solution defined in *Theorem 6.3*. Define the following mapping:

$$\begin{aligned}\Upsilon: U_{ad}&\to W^{1,2}(0,T;\mathcal{H}),\\ (v,\gamma)&\to \ell.\end{aligned}$$

To derive the first-order necessary conditions for the optimal controls, we prove the Gateaux differentiability of Υ on U_{ad}.

Let $\varepsilon>0$, $(v,\gamma)\in U_{ad}$ and $(v^\varepsilon,\gamma^\varepsilon)=(v^*,\gamma^*)+\varepsilon(v,\gamma)\in U_{ad}$. Let $\varrho^\varepsilon=\frac{1}{\varepsilon}(\ell^\varepsilon-\ell^*)$ where $\ell^\varepsilon=\Upsilon(v^\varepsilon,\gamma^\varepsilon)$ and $\ell^*=\Upsilon(v^*,\gamma^*)$. Then we get:

$$\begin{cases}\partial_t\varrho_1^\varepsilon=d_1\Delta\varrho_1^\varepsilon-\left(\beta\frac{\ell_3^\varepsilon(x,t-\zeta)}{1+\alpha\ell_3^\varepsilon(x,t-\zeta)}+\mu+v^\varepsilon\right)\varrho_1^\varepsilon+\lambda\varrho_5^\varepsilon\\ \qquad\qquad -\beta\ell_1^*E_3^\varepsilon(x,t-\zeta)\varrho_3^\varepsilon(x,t-\zeta)-\ell_1^*u,\\ \partial_t\varrho_2^\varepsilon=d_2\Delta\varrho_2^\varepsilon+v^\varepsilon\varrho_1^\varepsilon-\left(\delta\beta\frac{\ell_3^\varepsilon(x,t-\zeta)}{1+\alpha\ell_3^\varepsilon(x,t-\zeta)}+\mu\right)\varrho_2^\varepsilon\\ \qquad\qquad -\delta\beta\ell_2^*E_3^\varepsilon(x,t-\zeta)\varrho_3^\varepsilon(x,t-\zeta)+\ell_1^*u,\\ \partial_t\varrho_3^\varepsilon=d_3\Delta\varrho_3^\varepsilon+\beta\frac{\ell_3^\varepsilon(x,t-\zeta)}{1+\alpha\ell_3^\varepsilon(x,t-\zeta)}\varrho_1^\varepsilon+\delta\beta\frac{\ell_3^\varepsilon(x,t-\zeta)}{1+\alpha\ell_3^\varepsilon(x,t-\zeta)}\varrho_2^\varepsilon-(\mathrm{r}+\mu)\varrho_3^\varepsilon\ ;(x,t)\in\Xi\\ \qquad\qquad +\left(\beta\ell_1^*+\delta\beta\ell_2^*\right)E_3^\varepsilon(x,t-\zeta)\varrho_3^\varepsilon(x,t-\zeta),\\ \partial_t\varrho_4^\varepsilon=d_4\Delta\varrho_4^\varepsilon+r(1-\xi)\varrho_3^\varepsilon-(d+\mu+\gamma^\varepsilon)\varrho_4^\varepsilon-\ell_4^*\gamma,\\ \partial_t\varrho_5^\varepsilon=d_5\Delta\varrho_5^\varepsilon+r\xi\varrho_3^\varepsilon+\gamma^\varepsilon\varrho_4^\varepsilon-(\lambda+\mu)\varrho_5^\varepsilon+\ell_4^*\gamma,\end{cases}\tag{8.2}$$

where $E_3^\varepsilon(x,t-\zeta)=\left(\frac{\ell_3^\varepsilon(x,t-\zeta)}{1+\alpha\ell_3^\varepsilon(x,t-\zeta)}-\frac{\ell_3^*(x,t-\zeta)}{1+\alpha\ell_3^*(x,t-\zeta)}\right)\Big/(\ell_3^\varepsilon(x,t-\zeta)-\ell_3^*(x,t-\zeta))$,

$$\partial_\eta\varrho_1^\varepsilon=\partial_\eta\varrho_1^\varepsilon=\partial_\eta\varrho_1^\varepsilon=\partial_\eta\varrho_1^\varepsilon=\partial_\eta\varrho_1^\varepsilon=0\quad on\quad\partial\Omega\times[0,T]\,,\tag{8.3}$$

$$\varrho_1^\varepsilon=\varrho_2^\varepsilon=\varrho_3^\varepsilon=\varrho_4^\varepsilon=\varrho_5^\varepsilon=0\quad on\quad\Omega\times[0,T]\,.\tag{8.4}$$

We first prove that the solution of (8.2) is bounded. We need the following notations:

$$F_1^\varepsilon = \begin{pmatrix} \frac{-\beta\ell_3^\varepsilon(x,t-\zeta)}{1+\alpha\ell_3^\varepsilon(x,t-\zeta)} - \mu - v^\varepsilon & 0 & 0 & 0 & \lambda \\ v^\varepsilon & \frac{-\delta\beta\ell_3^\varepsilon(x,t-\zeta)}{1+\alpha\ell_3^\varepsilon(x,t-\zeta)} - \mu & 0 & 0 & 0 \\ \frac{\beta\ell_3^\varepsilon(x,t-\zeta)}{1+\alpha\ell_3^\varepsilon(x,t-\zeta)} & \frac{\delta\beta\ell_3^\varepsilon(x,t-\zeta)}{1+\alpha\ell_3^\varepsilon(x,t-\zeta)} & -r-\mu & 0 & 0 \\ 0 & 0 & r(1-\xi) & -d-\mu-\gamma^\varepsilon & 0 \\ 0 & 0 & r\xi & \gamma^\varepsilon & -\lambda-\mu \end{pmatrix},$$

$$F_2^\varepsilon = \begin{pmatrix} 0\,0 & -\beta\ell_1^* E_3^\varepsilon(x,t-\zeta) & 0\,0 \\ 0\,0 & -\delta\beta\ell_2^* E_3^\varepsilon(x,t-\zeta) & 0\,0 \\ 0\,0 & (\beta\ell_1^* + \delta\beta\ell_2^*)\, E_3^\varepsilon(x,t-\zeta) & 0\,0 \\ 0\,0 & 0 & 0\,0 \\ 0\,0 & 0 & 0\,0 \end{pmatrix},$$

$$F_3 = \begin{pmatrix} -\ell_1^* & 0 \\ \ell_1^* & 0 \\ 0 & 0 \\ 0 & -\ell_4^* \\ 0 & \ell_4^* \end{pmatrix},$$

to rewrite system (8.2) under the following compact form:

$$\begin{cases} \partial_t \varrho^\varepsilon = A\varrho^\varepsilon + F_1^\varepsilon(t)\varrho^\varepsilon(t) + F_2^\varepsilon(t)\varrho^\varepsilon(t-\zeta) + F_3(t)\left(v(t),\gamma(t)\right)^T, t \in [0,T], \\ \varrho^\varepsilon = 0 \quad on\ [-\zeta,0], \end{cases} \tag{8.5}$$

of which the unique solution, as seen before, is:

$$\begin{aligned} \varrho^\varepsilon(t) = &\int_0^t T(t-s)F_1^\varepsilon(s)\varrho^\varepsilon(s)ds + \int_0^t T(t-s)F_2^\varepsilon(s)\varrho^\varepsilon(s-\zeta)ds \\ &+ \int_0^t T(t-s)F_3(s)\left(v(t),\gamma(t)\right)^T ds, \end{aligned} \tag{8.6}$$

where $\{T(t),\ t \geq 0\}$ is the C_0 semigroup generated by the operator A. Using *Lemma* 8.1, one can show that there exist constants $M_6, M_7, M_8 \geq 0$ such that:

$$\begin{aligned} \|\varrho^\varepsilon(t)\|_{L^2(\Omega)} &\leq M_6 \int_0^t \|\varrho^\varepsilon(s)\|_{L^2(\Omega)} ds + M_7 \int_0^t \|\varrho^\varepsilon(s-\zeta)\|_{L^2(\Omega)} ds + M_8 \\ &\leq M_6 \int_0^t \|\varrho^\varepsilon(s)\|_{L^2(\Omega)} ds + M_7 \int_0^t \|\varrho^\varepsilon(s)\|_{L^2(\Omega)} ds + M_8 \\ &\leq M_8 + 2\,max(M_6, M_7) \int_0^t \|\varrho^\varepsilon(s)\|_{L^2(\Omega)} ds \end{aligned}$$

and applying Gronwall's inequality, we deduce the uniform boundedness of ϱ^{ε} in $L^2(\Xi)$. Furthermore, given that :

$$\|\ell_i^{\varepsilon} - \ell_i^*\|_{L^2(\Xi)} = \varepsilon \|\varrho_i^{\varepsilon}\|_{L^2(\Xi)}, \tag{8.7}$$

we can deduce that:

$$\ell^{\varepsilon} \underset{\varepsilon \to 0}{\to} \ell^* \ in \ L^2(\Xi).$$

Let F_1 and F_2 be two matrices defined by:

$$F_1 = \begin{pmatrix} \frac{-\beta \ell_3^*(x,t-\zeta)}{1+\alpha \ell_3^*(x,t-\zeta)} - \mu - v^* & 0 & 0 & 0 & \lambda \\ v^* & (\frac{-\delta\beta \ell_3^*(x,t-\zeta)}{1+\alpha \ell_3^*(x,t-\zeta)} - \mu & 0 & 0 & 0 \\ \frac{\beta \ell_3^*(x,t-\zeta)}{1+\alpha \ell_3^*(x,t-\zeta)} & \frac{\delta\beta \ell_3^*(x,t-\zeta)}{1+\alpha \ell_3^*(x,t-\zeta)} & -r-\mu & 0 & 0 \\ 0 & 0 & r(1-\xi) & -d-\mu-\gamma^* & 0 \\ 0 & 0 & r\xi & \gamma^* & -\lambda-\mu \end{pmatrix},$$

$$F_2 = \begin{pmatrix} 0\ 0 & \frac{-\beta \ell_1^*}{\left(1+\alpha \ell_3^*(x,t-\zeta)\right)^2} & 0\ 0 \\ 0\ 0 & \frac{-\delta\beta \ell_2^*}{\left(1+\alpha \ell_3^*(x,t-\zeta)\right)^2} & 0\ 0 \\ 0\ 0 & \frac{\beta \ell_1^* + \delta\beta \ell_2^*}{\left(1+\alpha \ell_3^*(x,t-\zeta)\right)^2} & 0\ 0 \\ 0\ 0 & 0 & 0\ 0 \\ 0\ 0 & 0 & 0\ 0 \end{pmatrix},$$

The solution of:

$$\begin{cases} \partial_t \varrho = A\varrho + F_1(t)\varrho(t) + F_2(t)\varrho(t-\zeta) + F_3(t)(v(t), \gamma(t))^T \quad , t \in [0,T], \\ \varrho = 0 \quad on\ [-\zeta, 0], \end{cases} \tag{8.8}$$

verifies:

$$\begin{aligned} \varrho(t) = &\int_0^t T(t-s)F_1(s)\varrho(s)ds + \int_0^t T(t-s)F_2(s)\varrho(s-\zeta)ds \\ &+ \int_0^t T(t-s)F_3(s)v^T(s)ds. \end{aligned} \tag{8.9}$$

From (8.6) and (8.9):

$$\begin{aligned} \varrho^{\varepsilon}(t) - \varrho(t) = &\int_0^t T(t-s)F_1^{\varepsilon}(s)\left(\varrho^{\varepsilon}(s) - \varrho(s)\right)ds \\ &+ \int_0^t T(t-s)F_2^{\varepsilon}(s)\left(\varrho^{\varepsilon}(s-\zeta) - \varrho(s-\zeta)\right)ds \\ &+ \int_0^t T(t-s)\left(F_1^{\varepsilon}(s) - F_1(s)\right)\varrho(s)ds \end{aligned}$$

$$
\begin{aligned}
&+\int_0^t T(t-s)\left(F_2^\varepsilon(s)-F_2(s)\right)\varrho(s-\zeta)ds\\
&=\int_0^t T(t-s)F_1^\varepsilon(s)\left(\varrho^\varepsilon(s)-\varrho(s)\right)ds\\
&+\int_{-\zeta}^{t-\zeta} T(t-s-\zeta)F_2^\varepsilon(s+\zeta)\left(\varrho^\varepsilon(s)-\varrho(s)\right)ds\\
&+\int_0^t T(t-s)\left(F_1^\varepsilon(s)-F_1(s)\right)\varrho(s)ds\\
&+\int_0^t T(t-s)\left(F_2^\varepsilon(s)-F_2(s)\right)\varrho(s-\zeta)ds.
\end{aligned}
$$

F_1^ε and F_2^ε are uniformly bounded with respect to ε in Ξ and tend to F_1 and F_2 when $\varepsilon\to 0$. By applying Gronwall's inequality, we get:

$$\varrho^\varepsilon \underset{\varepsilon\to 0}{\to} \varrho \quad in \quad L^2(\Xi). \tag{8.10}$$

Moreover,

$$\varrho = \Upsilon'((v^*,\gamma^*))(v,\gamma). \tag{8.11}$$

Theorem 8.1. *The functional J defined in (5.4) is Gateaux differentiable in U_{ad}. Furthermore, if (ℓ^*,u^*,γ^*) is an optimal triplet, then the adjoint problem:*

$$\begin{cases}\partial_t\rho = -A\rho - F_1^*(t)\rho(t) - 1_{[0;T-\zeta]}(t)F_2^*(t+\zeta)\rho(t+\zeta) - K\\ \rho(x,T)=0\end{cases}, t\in[0,T] \tag{8.12}$$

associated to (5.1)-(5.4), where $K=\begin{pmatrix}\kappa_1,\,0,\,\kappa_2,\,\kappa_3,\,0\end{pmatrix}^T$ and, for any set X, $1_X(.)$ is the indicator function of the set X, has a unique solution $\rho=(\rho_1,\rho_2,\rho_3,\rho_4,\rho_5)^T\in W^{1,2}(0,T;\mathcal{H})$ with $\rho_i\in L^2(0,T;H^2(\Omega))\cap L^\infty(0,T;H^1(\Omega))$ for $i=1,2,3,4,5$. In addition:

$$\begin{cases}v^* = \min\left(v_{\max},\max\left(0,\frac{S^*}{\alpha_1}(\rho_1-\rho_2)\right)\right),\\ \gamma^* = \min\left(\gamma_{\max},\max\left(0,\frac{I_s^*}{\alpha_2}(\rho_4-\rho_5)\right)\right).\end{cases} \tag{8.13}$$

Proof. *STEP 1* Let $t'=T-t$ and $v_i(t',x)=\rho_i(T-t',x)=\rho_i(x,t)$ for $(x,t)\in\Xi$. Following a reasoning similar to the proof in [16], we deduce the first part.

STEP 2 Let (ℓ^*,v^*,γ^*) be an optimal triplet and let $\ell^\varepsilon=(\ell_1^\varepsilon,\ell_2^\varepsilon,\ell_3^\varepsilon,\ell_4^\varepsilon,\ell_5^\varepsilon)=\Upsilon(v^\varepsilon,\gamma^\varepsilon)$ where $(v^\varepsilon,\gamma^\varepsilon)=(v^*,\gamma^*)+\varepsilon(v,\gamma)\in U_{ad}$. We get the following:

$$
\begin{aligned}
J'(v^*,\gamma^*)(v,\gamma) &= \lim_{\varepsilon\to 0}\frac{1}{\varepsilon}\left(J(v^\varepsilon,\gamma^\varepsilon)-J(v^*,\gamma^*)\right)\\
&=\lim_{\varepsilon\to 0}\frac{1}{\varepsilon}\left(\int_0^T\int_\Omega\left[\kappa_1(\ell_1^\varepsilon-\ell_1^*)+\kappa_2(\ell_3^\varepsilon-\ell_3^*)+\kappa_3(\ell_4^\varepsilon-\ell_4^*)\right]dxdt\right.\\
&\left.+\frac{\alpha_1}{2}\int_0^T\int_\Omega\left[(v^\varepsilon)^2-(v^*)^2\right]dxdt+\frac{\alpha_2}{2}\int_0^T\int_\Omega\left[(\gamma^\varepsilon)^2-(\gamma^*)^2\right]dxdt\right)\\
&=\int_0^T\int_\Omega\left[\kappa_1\varrho_1+\kappa_2\varrho_3+\kappa_3\varrho_4\right]dxdt+\int_0^T\int_\Omega\left[\alpha_1 vv^*+\alpha_2\gamma\gamma^*\right]dxdt
\end{aligned}
$$

$$
\begin{aligned}
&= \int_0^T \langle K, \varrho \rangle_{\mathcal{H}} dt + \int_0^T \langle (\alpha_1 v^*, \alpha_2 \gamma^*)^T, (v, \gamma)^T \rangle_{(L^2(\Omega))^2} dt \\
&= \int_0^T \langle \rho, \frac{\partial \varrho}{\partial t} - A\varrho - F_1(t)\varrho(t) - F_2(t)\varrho(t-\zeta) \rangle_{\mathcal{H}} dt \\
&+ \int_0^T \langle (\alpha_1 v^*, \alpha_2 \gamma^*)^T, (v, \gamma)^T \rangle_{(L^2(\Omega))^2} dt \\
&= \int_0^T \langle \rho, F_3 (v, \gamma)^T \rangle_{\mathcal{H}} dt + \int_0^T \langle (\alpha_1 v^*, \alpha_2 \gamma^*)^T, (v, \gamma)^T \rangle_{(L^2(\Omega))^2} dt \\
&= \int_0^T \langle F_3^* \rho, (v, \gamma)^T \rangle_{(L^2(\Omega))^2} dt + \int_0^T \langle (\alpha_1 v^*, \alpha_2 \gamma^*)^T, (v, \gamma)^T \rangle_{(L^2(\Omega))^2}.
\end{aligned}
$$

We deduce the characterizations of v^* and γ^*:

$$
v^* = \min\left(v_{\max}, \max\left(0, \frac{S^*}{\alpha_1}(\rho_1 - \rho_2)\right)\right),
$$

$$
\gamma^* = \min\left(\gamma_{\max}, \max\left(0, \frac{I_s^*}{\alpha_2}(\rho_4 - \rho_5)\right)\right).
$$

□

9. Simulation results

9.1. Parameter values and model simulation

To solve the COVID-19 epidemic model, we utilize the finite difference method (FDM) and the forward-backward sweep approach [28], enabling numerical approximation of the model's partial differential equations. The FDM approximates derivatives at discrete grid points, transforming the governing equations into a system of algebraic equations that can be solved numerically. For spatial discretization, the spatial domain is divided into a grid with uniform spacing (Δx) and (Δy), while the temporal domain is discretized with a time step (Δt), employing the forward Euler method for time integration. The forward-backward sweep method consists of three main steps. In the **forward sweep**, we solve the state equations from the initial time $(t = 0)$ to the final time $(t = T)$, generating the trajectory of state variables across time and space. Here, control variables—vaccination v and hospitalization γ are applied according to the model dynamics to influence the spread of the infection. The **backward sweep** then involves solving the adjoint equations in reverse from $(t = T)$ back to $(t = 0)$, using results from the forward pass to inform adjustments in control variables. This iterative process leverages gradients obtained from the adjoint equations to refine the control strategies, aiming to minimize the density of susceptible, infected, and severe cases while meeting convergence criteria (such as tolerance levels, maximum iterations, and cost function evaluations). For a practical illustration, we simulate COVID-19 propagation over a (60 km $\times$ 50 km) region, assuming initial infections occur at two specific locations: $(\Omega_1 = \text{cell}(45, 30))$ and $(\Omega_2 = \text{cell}(2, 2))$. The controlled and uncontrolled epidemic scenarios are simulated over 180 days, with intervention measures implemented from day 30 onward. Tables 2 and 4 provide the specific parameter values used for the simulations.

Table 3 shows the summary of infected individuals with no severe symptoms, severe cases, and total deaths by the end of our simulations.

Compartment	Initial Value
Susceptibles	$450\ for\ x \in \Omega_i \quad and \quad 500\ for\ x \notin \Omega_i\ , \quad i = 1, 2$
Vaccinated	$0\ for\ x \in \Omega_i \quad and \quad 0\ for\ x \notin \Omega_i\ , \quad i = 1, 2$
Infected	$40\ for\ x \in \Omega_i \quad and \quad 0\ for\ x \notin \Omega_i\ , \quad i = 1, 2$
Severe cases	$10\ for\ x \in \Omega_i \quad and \quad 0\ for\ x \notin \Omega_i\ , \quad i = 1, 2$
Recovered	$0\ for\ x \in \Omega_i \quad and \quad 0\ for\ x \notin \Omega_i\ , \quad i = 1, 2$
Total	1500000

Table 2. Initial population distribution

Scenario	Infected (I)	Severe cases (I_s)	Deaths	Cost
Without control	41433	164345	324452	0
Hospitalization	55697	29387	84246	632179493
Vaccination	31573	106584	171290	35048016
Both controls	36766	20065	43324	356899817

Table 3. Simulation results of infected individuals with no severe symptoms, severe cases, and total deaths for the different scenarios by day 180

9.2. Interpretation of results

Without intervention, the virus spreads across all regions, leading to a rapid escalation in the density of severe cases. By day 180, the cumulative death toll reaches 324,452.

To evaluate the comparative effectiveness of vaccination and hospitalization as control strategies, we consider three distinct scenarios. In the first scenario, patients with severe symptoms receive hospitalization, factoring in the limitations of healthcare resources and bed capacity. This approach results in a substantial decrease in the density of severe cases, ultimately preventing approximately 240,206 deaths.

In the second scenario, vaccination is implemented as the sole intervention. Numerical simulations indicate that while this strategy is more cost-effective, it is less impactful in reducing severe cases and mortality, as it lacks targeted treatment for individuals with severe symptoms.

Lastly, the combined application of both vaccination and hospitalization yields the most favorable outcomes. This integrated approach not only proves to be more cost-effective than relying on hospitalization alone but also significantly reduces both the number of severe cases and fatalities, demonstrating the benefits of a multifaceted control strategy.

Parameter	Value	Reference
ζ	5 days	[48]
α	0.15 day	[49]
β	0.0115	[31]
$1-\delta$	0.8	assumed
ξ	0.8 day^{-1}	[42]
r	0.222 day^{-1}	[30, 41]
Π	$\frac{1500000}{70\times365}$ $\text{people.day}^{-1}.\text{km}^{-2}$	[13]
μ	$\frac{1}{70\times365}$ day^{-1}	[17]
d	0.014 day^{-1}	[40]
λ	0.011 day^{-1}	[37]
v_{max}	0.5	assumed
γ_{max}	0.071	[40]
α_1, α_2	20, 1500	[6, 26]
κ_1,κ_2,κ_3	$1, 1.5, 1.5$	assumed
d_1,d_2,d_3,d_5	0.5 $km^2.\text{day}^{-1}$	assumed
d_4	0.1 $km^2.\text{day}^{-1}$	assumed

Table 4. Parameters used in the simulations

9.2.1. Without control strategy

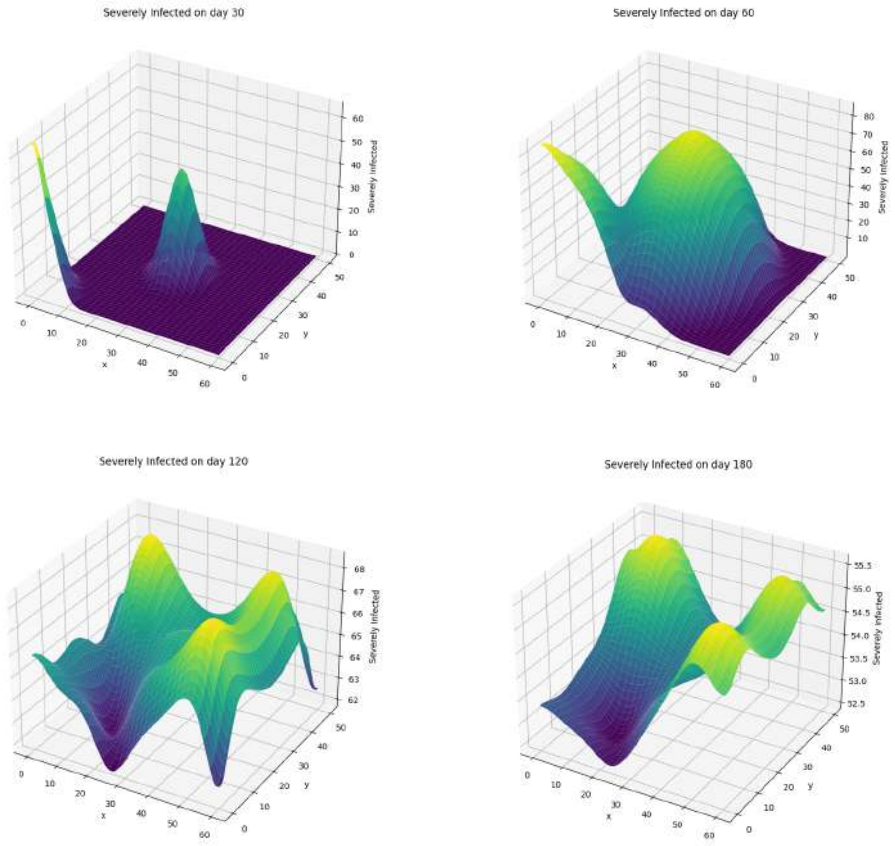

Figure 1. Severely infected population I_s dynamics through time and space when no strategy is used.

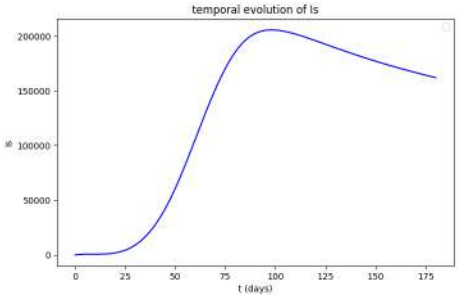

Figure 2. Temporal evolution of I_s when no strategy is used.

9.2.2. Hospitalization

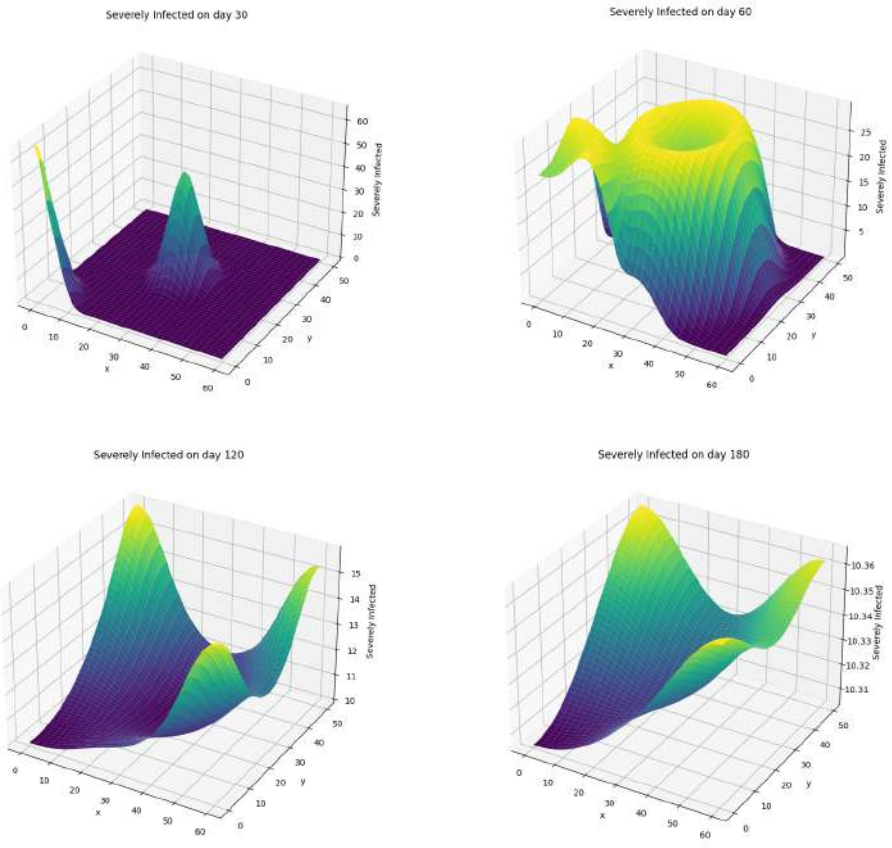

Figure 3. Severely infected population I_s dynamics through time and space when we rely only on hospitalization.

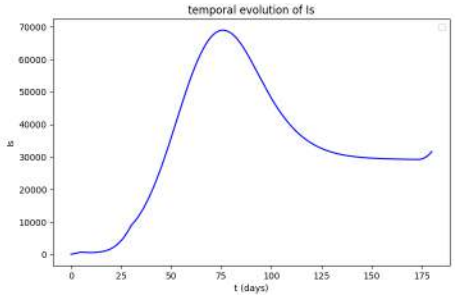

Figure 4. Temporal evolution of I_s when we rely only on hospitalization.

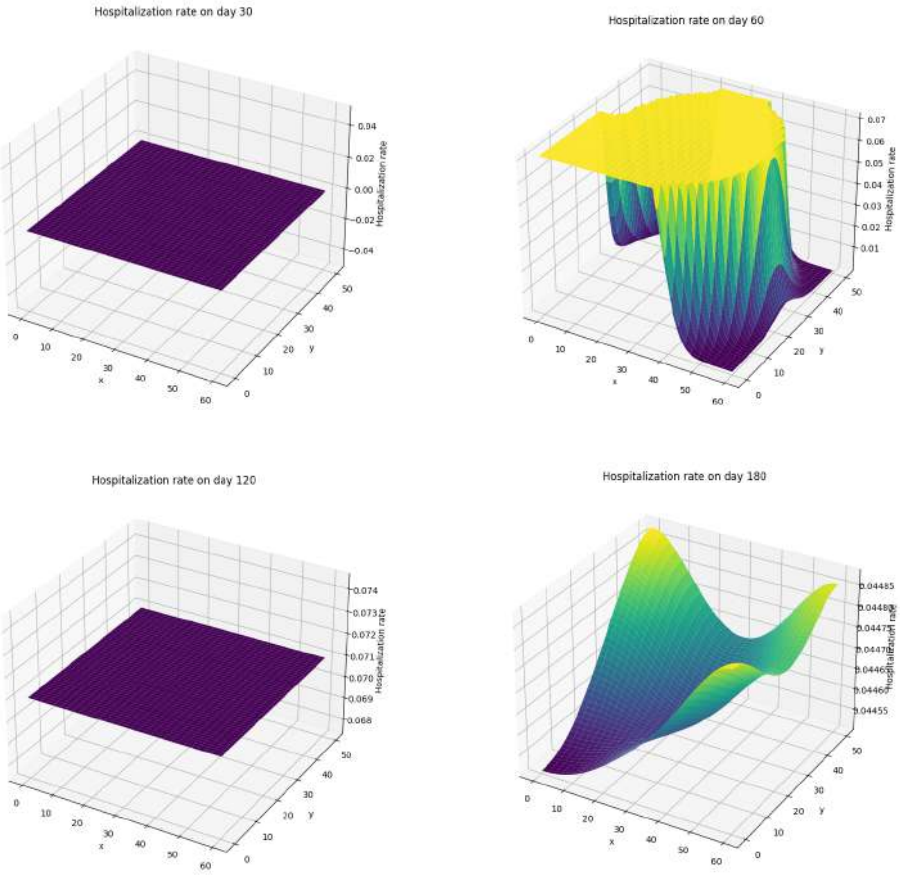

Figure 5. Hospitalization rate γ through time and space when we rely only on hospitalization.

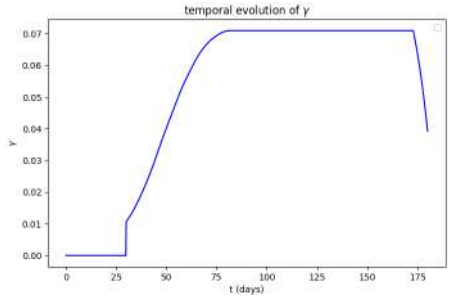

Figure 6. Temporal evolution of γ when we rely only on hospitalization.

9.2.3. Vaccination

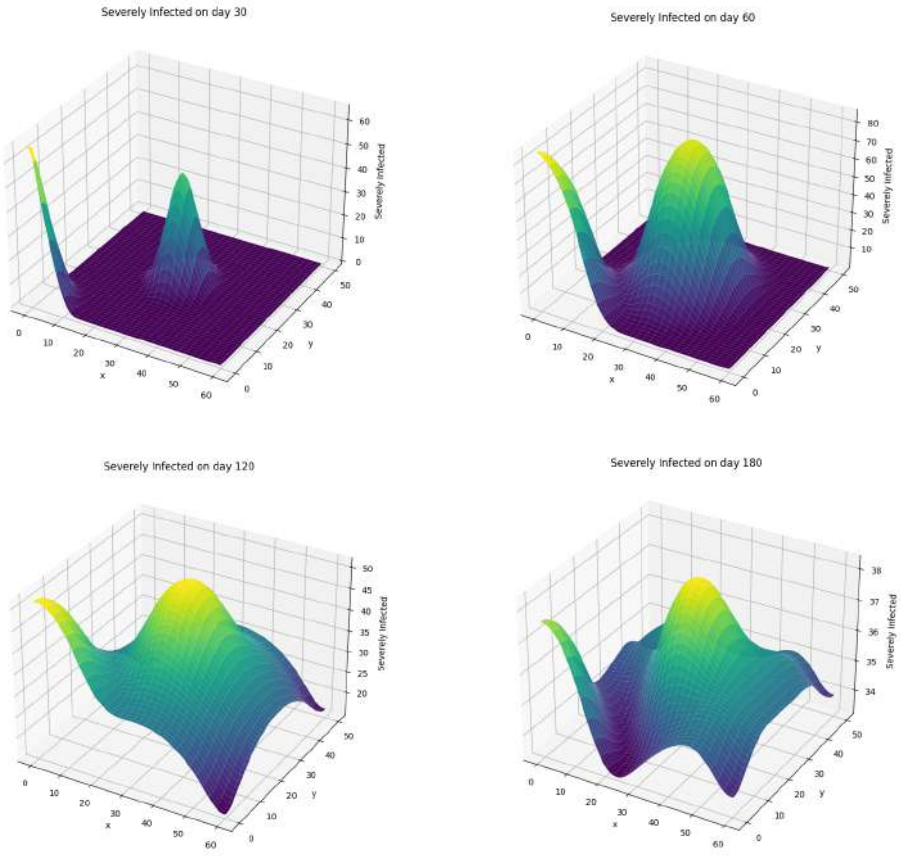

Figure 7. Severely infected population I_s dynamics through time and space when we rely only on vaccination.

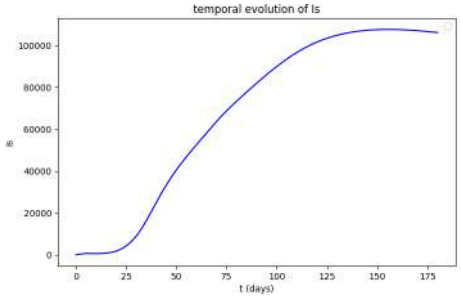

Figure 8. Temporal evolution of I_s when we rely only on vaccination.

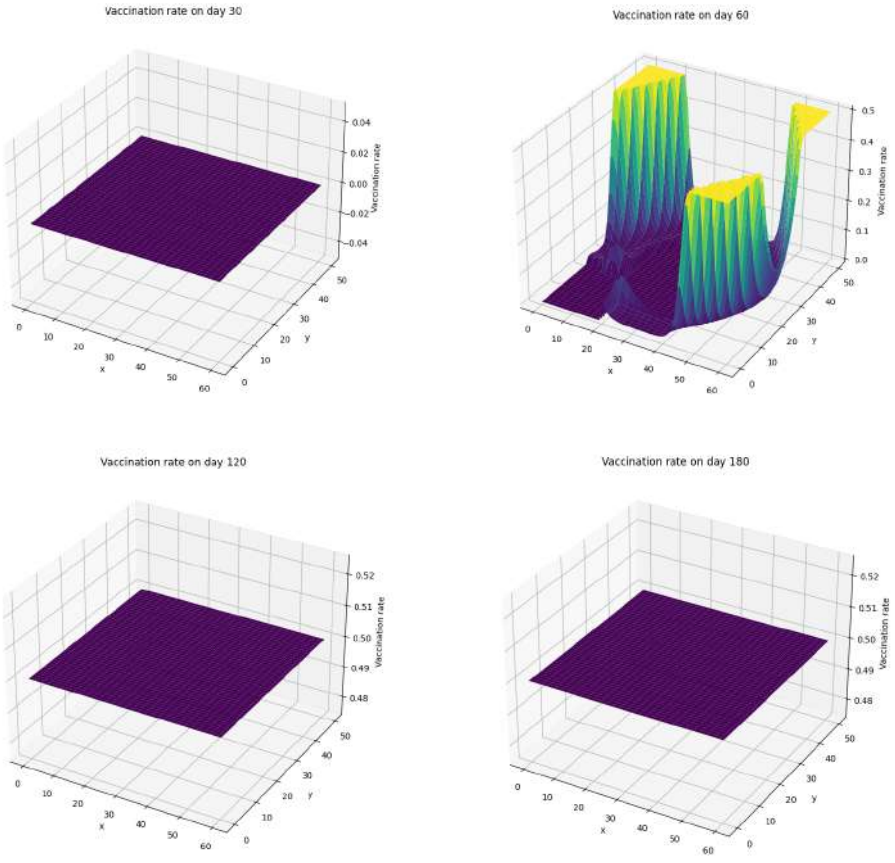

Figure 9. Vaccination rate v through time and space when we rely only on vaccination.

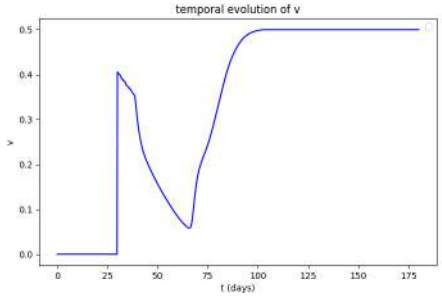

Figure 10. Temporal evolution of vaccination rate v when we rely only on vaccination.

9.2.4. Both control strategies

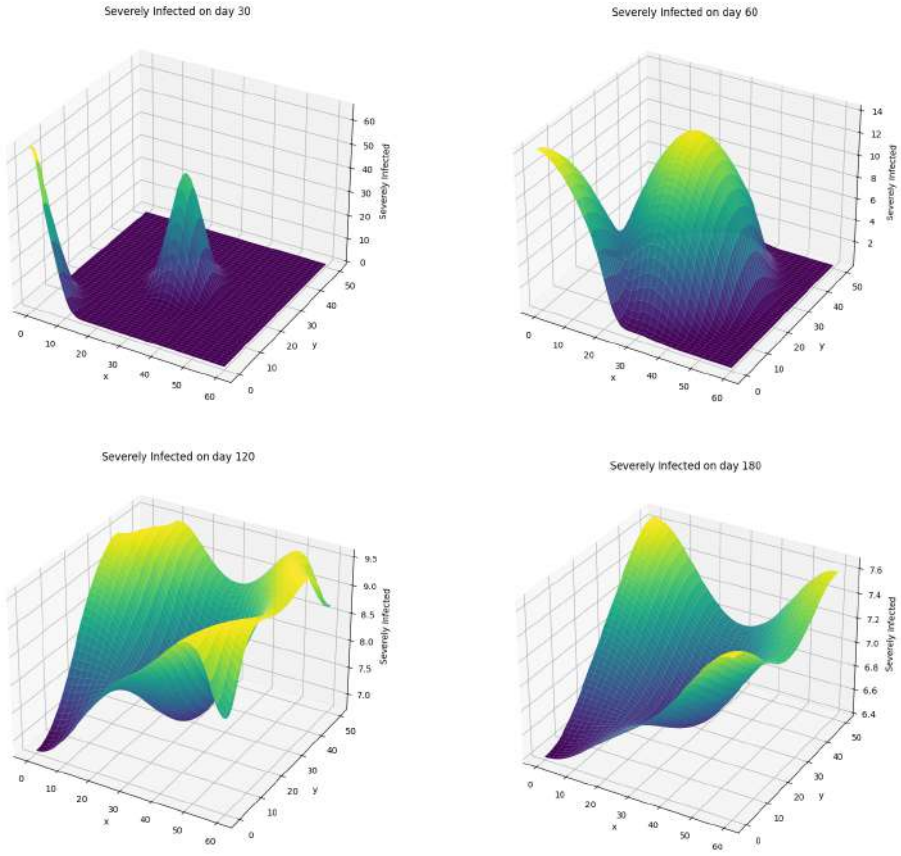

Figure 11. Severely infected population I_s dynamics through time and space when we use both strategies simultaneously.

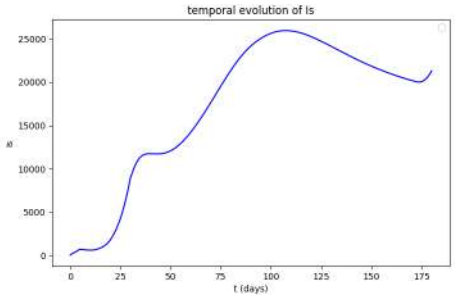

Figure 12. Temporal evolution of I_s when we use both strategies simultaneously.

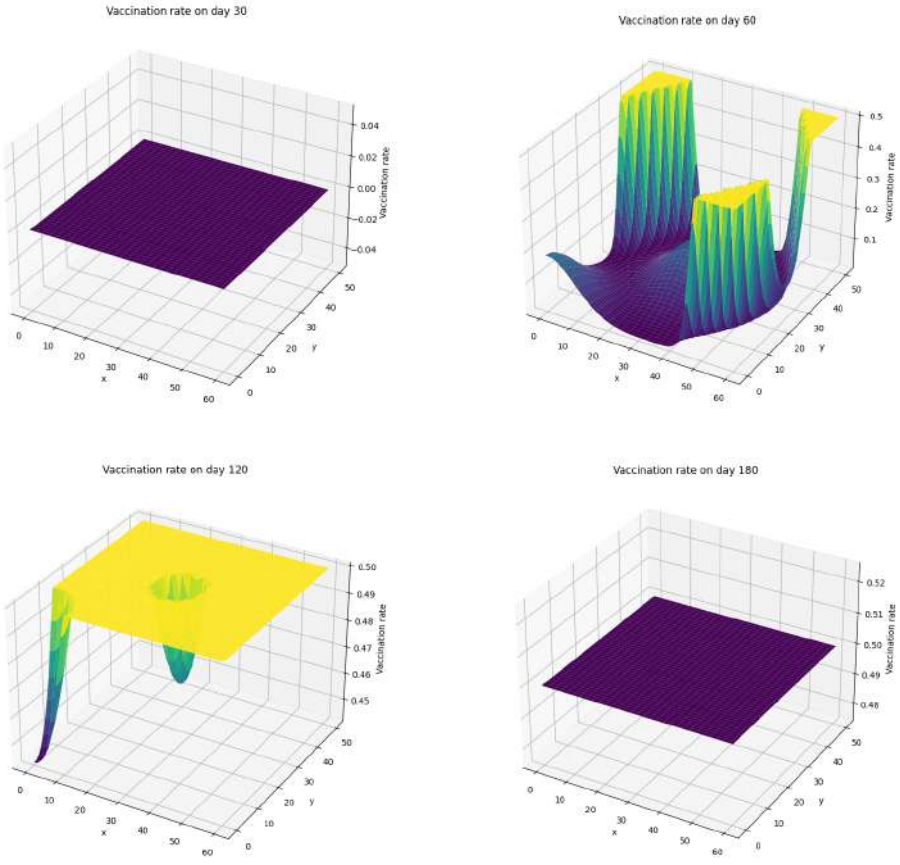

Figure 13. Vaccination rate v through time and space when we use both strategies simultaneously.

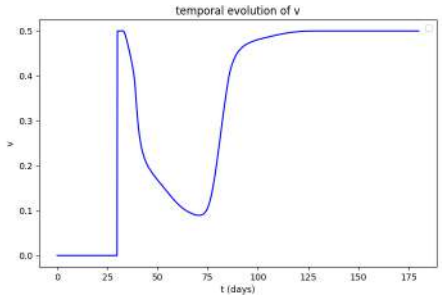

Figure 14. Temporal evolution of v when we use both strategies simultaneously.

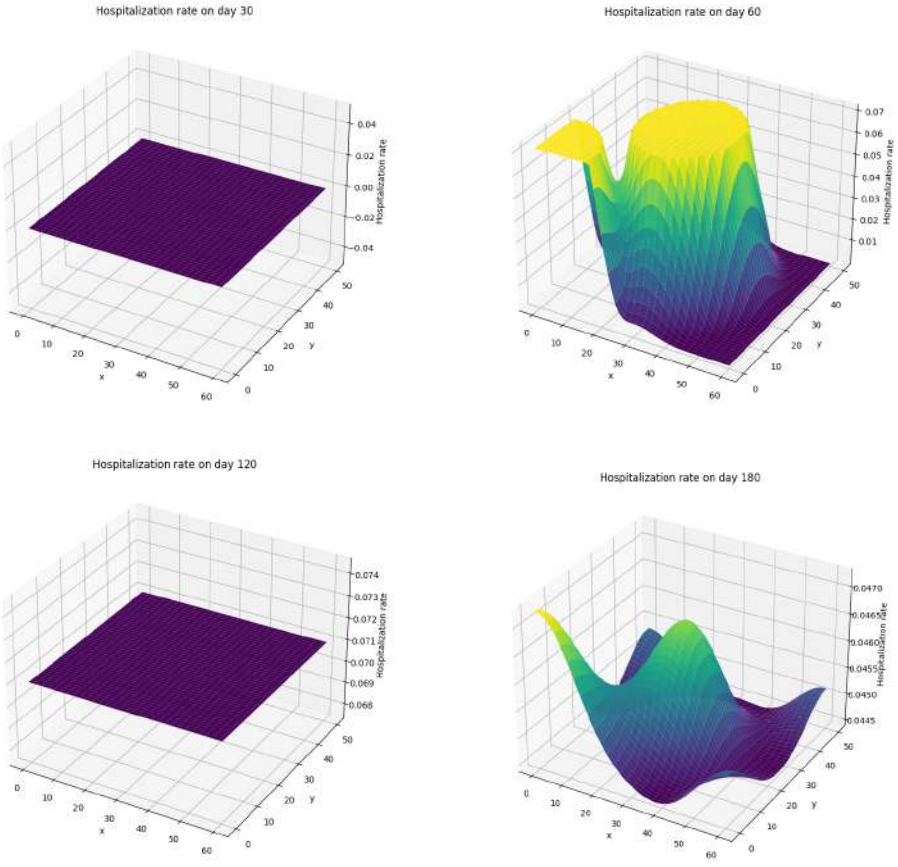

Figure 15. Hospitalization rate γ through time and space when we use both strategies simultaneously.

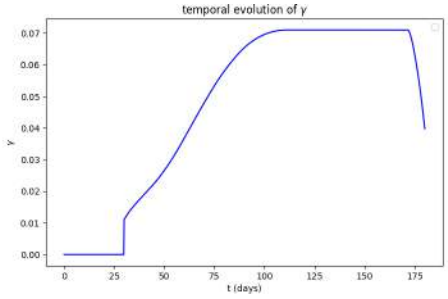

Figure 16. Temporal evolution of γ when we use both strategies simultaneously.

9.3. Model response to parameter modifications

To further investigate the model's responsiveness to changes in key parameters, we examine the effects of varying the saturation rate α, highest feasible rate of vaccination v_{max} and highest feasible rate of hospitalization γ_{max}. By adjusting these parameters to specific, plausible values, we aim to observe the resulting dynamics

in infection spread, control effectiveness, and healthcare demand. This approach allows us to test how variations in α, v_{max} and γ_{max} influence model behavior in both controlled and uncontrolled epidemic scenarios, providing insights into how flexible control strategies may better adapt to real-world conditions.

9.3.1. Increased hospitalization and vaccination capacity

This subsection explores the effects of increasing the maximum hospitalization rate, γ_{max}, and the maximum vaccination rate, v_{max}, on infection control and severe case outcomes. By simulating scenarios with enhanced capacity, we aim to assess the potential for reducing severe cases and mortality under higher intervention capabilities. Key findings include:

- Enhanced Containment of Severe Cases: Increasing γ_{max} allows for a greater number of individuals with severe symptoms to receive timely care, resulting in a substantial decrease in the density of severe cases. This, in turn, significantly reduces overall mortality, while avoiding any significant increase in costs, by improving treatment accessibility during peak infection periods.

- Impact on Infection Dynamics: Higher v_{max} accelerates the vaccination rollout, which quickly boosts immunity in the population. This faster immunization rate effectively lowers transmission rates, thereby decreasing the infection spread more rapidly compared to scenarios with lower vaccination rates.

- Synergistic Effects: The simultaneous enhancement of both $gamma_{max}$ and v_{max} offers the best outcomes, as it combines immediate treatment for severe cases with preventive immunization. This dual approach significantly reduces the overall infection burden while maintaining cost-efficiency by limiting the progression to severe cases and accelerating the decline of the susceptible population.

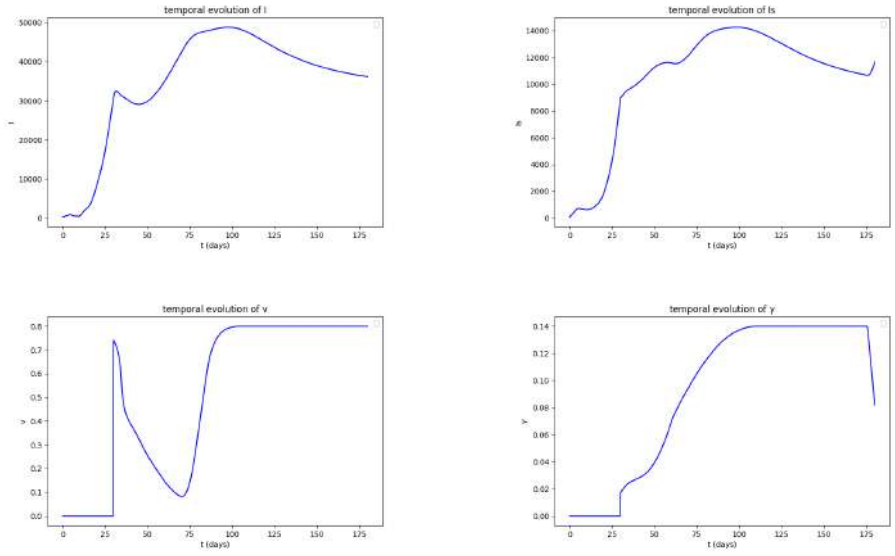

Figure 17. Temporal evolution of I, I_s, v, and γ when we use both strategies simultaneously with $\alpha = 0.15$, $v_{max} = 0.8$, and $\gamma_{max} = 0.14$

Scenario	Infected (I)	Severe cases (I_s)	Deaths	Cost
Without control	41433	164345	324452	0
Hospitalization	57525	16594	49387	718160376
Vaccination	31092	105371	170155	35377789
Both controls	36500	10680	26414	403734701

Table 5. Simulation results of infected individuals with no severe symptoms, severe cases, and total deaths for the different scenarios by day 180 with $\alpha = 0.15$, $v_{max} = 0.8$, and $\gamma_{max} = 0.14$

9.3.2. Effects of elevated saturation rate

This subsection examines the impact of increasing the saturation rate α in the Holling type-II functional response, which influences the interaction between the susceptible and infected populations. The saturation rate α represents the rate at which the functional response diminishes as the infected population increases. Varying this parameter allows us to understand how it affects the epidemic dynamics, particularly the spread of the infection and the burden on the healthcare system.

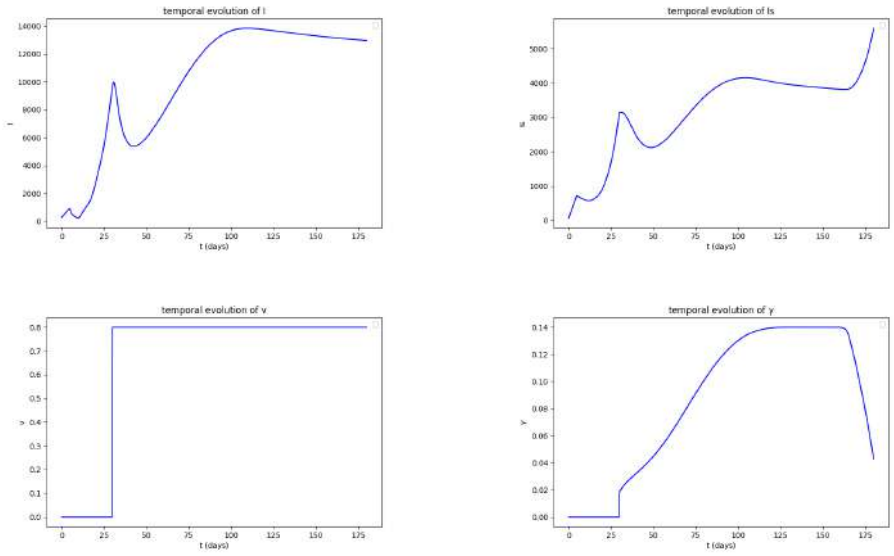

Figure 18. Temporal evolution of I, I_s, v, and γ when we use both strategies simultaneously with $\alpha = 0.8$, $v_{max} = 0.8$, and $\gamma_{max} = 0.14$.

- Increased Infection Control Efficiency: A higher saturation rate α implies that the transmission rate becomes less sensitive to increases in the infected population. This results in a more efficient control of the epidemic and leads to a reduction in the overall number of infections over time, making it easier to manage the epidemic with available healthcare resources.

- Impact on Intervention Strategies: Increasing α can also alter the effectiveness

of vaccination and hospitalization strategies. While higher saturation rate may reduce the overall burden of the infection, the timing and scale of interventions must be adjusted to account for possible extended duration of the epidemic.

Scenario	Infected (I)	Severe cases (I_s)	Deaths	Cost
Without control	35794	120598	180246	0
Hospitalization	40746	11885	28434	411453332
Vaccination	12670	34434	44423	32729792
Both controls	13013	4612	7946	134223251

Table 6. Simulation results of infected individuals with no severe symptoms, severe cases, and total deaths for the different scenarios by day 180 with $\alpha = 0.8$, $v_{max} = 0.8$, and $\gamma_{max} = 0$.

10. Conclusion

In this study, we developed a delayed spatiotemporal epidemic model with a Holling type-II saturated incidence rate, applicable to epidemics such as SARS and COVID-19. The model incorporates features like temporary immunity, vital dynamics, vaccination, and hospitalization. We established the model's mathematical and biological well-posedness and demonstrated that the basic reproduction number R_0 determines the local stability of the disease-free equilibrium: it is stable if $R_0 \leq 1$ and unstable if $R_0 > 1$. For a latent period ζ, we derived the conditions for asymptotic stability of an endemic equilibrium if $\zeta = 0$, and we demonstrated that this equilibrium is asymptotically stable independently of ζ when $\zeta > 0$ and some inequalities hold. We formulated an optimal control problem to minimize epidemic spread and associated costs through vaccination and hospitalization rates dependent on both time and spatial location. Existence and uniqueness of solutions were demonstrated, along with first-order necessary conditions and optimal solution characterizations.

Using COVID-19 as a case study, we derived numerical simulations under various scenarios. Results demonstrated that integrating spatial and temporal factors with the latent period allows targeted vaccination and hospitalization strategies to minimize severe cases and fatalities cost-effectively. Unlike traditional temporal models, it is also possible to control the rate of vaccination and hospitalization by region or area that needs more or less attention to get the best possible results.

A comparison of control strategies revealed that combining vaccination and hospitalization yields the most effective results, followed by vaccination alone. Additional preventive measures, such as social distancing and mask-wearing, can further support epidemic control.

Key findings from this study underscore the advantage of spatially optimized interventions. Targeting high-risk areas with vaccination and hospitalization not only improves public health outcomes but also enhances resource allocation, reducing costs and inefficiencies. Spatially adaptive approaches prevent the overspending seen in uniform temporal models, addressing high-risk regions more precisely.

The implications extend to healthcare resource management, aiding policymakers in predicting and managing hospital demand to avoid overwhelming facilities. Cost-effectiveness emerges as a crucial advantage, offering an economically sustainable framework for epidemic response. Public awareness campaigns can leverage these findings to emphasize vaccination's role in reducing transmission and enhancing compliance.

To translate these findings into policy, we recommend establishing real-time data systems for monitoring vaccination impacts and hospital utilization, fostering collaboration with local health agencies for targeted campaigns, and regularly reviewing strategies in response to evolving data.

For future research, we propose:

- Time-Varying Transmission Rates: Incorporate dynamic transmission rates informed by real-time data, especially in response to variant emergence.
- Spatially Variable Maximal Rates: Enable region-specific maximal rates for vaccination and hospitalization to adapt interventions by area.
- Behavioral Factors: Account for public compliance and psychological factors influencing vaccination uptake and hospitalization adherence.
- Broader Healthcare Context: Expand the model to include healthcare resource constraints, allowing holistic management of medical supplies, workforce, and patient flow.
- Spatial Heterogeneity and Network Dynamics: Model urban-rural transmission patterns and social network effects to capture nuanced spatial spread.
- Long-Term Immunity Dynamics: Extend immunity modeling to include waning and booster effects for sustainable immunity.
- Empirical Validation and Real-World Collaboration: Validate model predictions with empirical data and collaborate with health authorities to implement pilot interventions.

Acknowledgements

The authors sincerely thank the reviewers for their valuable time, constructive feedback, and insightful suggestions, which significantly contributed to enhancing the quality of this paper.

References

[1] A. Abidemi, Z. M. Zainuddin and N. A. B. Aziz, *Impact of control interventions on covid-19 population dynamics in malaysia: a mathematical study*, The European Physical Journal Plus, 2021, 136(2), 1-35.

[2] K. Adnaoui and A. El Alami Laaroussi, *An optimal control for a two-dimensional spatiotemporal seir epidemic model*, International Journal of Differential Equations, 2020, 2020.

[3] K. Adnaoui, I. Elberrai, A. E. A. Laaroussi and K. Hattaf, *A spatiotemporal sir epidemic model two dimensional with problem of optimal control*, Boletim da Sociedade Paranaense de Matemática, 2022, 40, 1-18.

[4] A. Alabkari, K. Adnaoui, A. Kourrad and A. Bennar, *Optimal control of a community violence model: community violence treated as a contagious disease*, Commun. Math. Biol. Neurosci., 2021.

[5] A. Alabkari, A. Kourrad, K. Adnaoui et al., *Control of a reaction-diffusion system: application on a seir epidemic model*, J. Math. Comput. Sci., 2021, 11(2), 1601-1628.

[6] N. J. Alvis-Zakzuk, Á. Flórez-Tanus, D. Díaz-Jiménez et al., *How expensive are hospitalizations by covid-19? evidence from colombia*, Value in health regional issues, 2022, 31, 127-133.

[7] Z. Bai and S.-L. Wu, *Traveling waves in a delayed sir epidemic model with nonlinear incidence*, Applied Mathematics and Computation, 2015, 263, 221-232.

[8] V. Barbu, *Mathematical methods in optimization of differential systems*, 310, Springer Science & Business Media, 2012.

[9] E. B. Bashier and K. C. Patidar, *Optimal control of an epidemiological model with multiple time delays*, Applied Mathematics and Computation, 2017, 292, 47-56.

[10] M. H. A. Biswas, L. T. Paiva, M. D. R. de Pinho et al., *A seir model for control of infectious diseases with constraints*, Mathematical Biosciences and Engineering, 2014, 11(4), 761-784.

[11] E. Bonyah, K. Badu and S. K. Asiedu-Addo, *Optimal control application to an ebola model*, Asian Pacific Journal of Tropical Biomedicine, 2016, 6(4), 283-289.

[12] F. E. Browder, *Non-linear equations of evolution*, Annals of Mathematics, 1964, 485-523.

[13] B. Chhetri, D. Vamsi and C. B. Sanjeevi, *Optimal control studies on age structured modeling of covid-19 in presence of saturated medical treatment of holling type iii*, Differential Equations and Dynamical Systems, 2022, 1-40.

[14] M. Diagne, H. Rwezaura, S. Tchoumi and J. Tchuenche, *A mathematical model of covid-19 with vaccination and treatment*, Computational and Mathematical Methods in Medicine, 2021, 2021.

[15] K. Dietz, *The first epidemic model: a historical note on pd en'ko*, Australian Journal of Statistics, 1988, 30(1), 56-65.

[16] A. El-Alami Laaroussi, M. Rachik and M. Elhia, *An optimal control problem for a spatiotemporal sir model*, International Journal of Dynamics and Control, 2018, 6(1), 384-397.

[17] Z. Feng and J. X. Velasco-Hernández, *Competitive exclusion in a vector-host model for the dengue fever*, Journal of mathematical biology, 1997, 35(5), 523-544.

[18] H. W. Hethcote, *The mathematics of infectious diseases*, SIAM review, 2000, 42(4), 599-653.

[19] Z. Jiang, W. Ma and J. Wei, *Global hopf bifurcation and permanence of a delayed seirs epidemic model*, Mathematics and Computers in Simulation, 2016, 122, 35-54.

[20] W. O. Kermack and A. G. McKendrick, *A contribution to the mathematical theory of epidemics*, Proceedings of the royal society of london. Series A, Containing papers of a mathematical and physical character, 1927, 115(772), 700-721.

[21] A. Kourrad, A. Alabkari, K. Adnaoui et al., *A spatiotemporal model with optimal control for the novel coronavirus epidemic in wuhan, china*, Commun. Math. Biol. Neurosci., 2021.

[22] A. Kourrad, A. Alabkari, A. Labriji et al., *Optimal control strategy with delay in state and control variables of transmission of covid-19 pandemic virus*, Commun. Math. Biol. Neurosci., 2020.

[23] M. U. Kraemer, C.-H. Yang, B. Gutierrez et al., *The effect of human mobility and control measures on the covid-19 epidemic in china*, Science, 2020, 368(6490), 493-497.

[24] A. Kumar, K. Goel et al., *A deterministic time-delayed sir epidemic model: mathematical modeling and analysis*, Theory in biosciences, 2020, 139(1), 67-76.

[25] H. Laarabi, A. Abta and K. Hattaf, *Optimal control of a delayed sirs epidemic model with vaccination and treatment*, Acta biotheoretica, 2015, 63(2), 87-97.

[26] D. W. Light and J. Lexchin, *The costs of coronavirus vaccines and their pricing*, Journal of the Royal Society of Medicine, 2021, 114(11), 502-504.

[27] Q. Liu, M. Sun and T. Li, *Analysis of an sirs epidemic model with time delay on heterogeneous network*, Advances in Difference Equations, 2017, 2017(1), 1-13.

[28] M. McAsey, L. Mou and W. Han, *Convergence of the forward-backward sweep method in optimal control*, Computational Optimization and Applications, 2012, 53(1), 207-226.

[29] D. V. Mehrotra, H. E. Janes, T. R. Fleming et al., *Clinical endpoints for evaluating efficacy in covid-19 vaccine trials*, Annals of internal medicine, 2021, 174(2), 221-228.

[30] S. S. Musa, S. Qureshi, S. Zhao et al., *Mathematical modeling of covid-19 epidemic with effect of awareness programs*, Infectious disease modelling, 2021, 6, 448-460.

[31] S. Mwalili, M. Kimathi, V. Ojiambo et al., *Seir model for covid-19 dynamics incorporating the environment and social distancing*, BMC Research Notes, 2020, 13(1), 1-5.

[32] F. Ndaïrou, I. Area, J. J. Nieto and D. F. Torres, *Mathematical modeling of covid-19 transmission dynamics with a case study of wuhan*, Chaos, Solitons & Fractals, 2020, 135, 109846.

[33] A. Omame, H. Rwezaura, M. Diagne et al., *Covid-19 and dengue co-infection in brazil: optimal control and cost-effectiveness analysis*, The European Physical Journal Plus, 2021, 136(10), 1-33.

[34] S. Ruan and J. Wei, *On the zeros of transcendental functions with applications to stability of delay differential equations with two delays*, Dynamics of Continuous Discrete and Impulsive Systems Series A, 2003, 10, 863-874.

[35] P. Samui, J. Mondal and S. Khajanchi, *A mathematical model for covid-19 transmission dynamics with a case study of india*, Chaos, Solitons & Fractals, 2020, 140, 110173.

[36] T. Sardar, S. Rana and J. Chattopadhyay, *A mathematical model of dengue transmission with memory*, Communications in Nonlinear Science and Numerical Simulation, 2015, 22(1-3), 511-525.

[37] M. Q. Shakhany and K. Salimifard, *Predicting the dynamical behavior of covid-19 epidemic and the effect of control strategies*, Chaos, Solitons & Fractals, 2021, 146, 110823.

[38] J. Simon, *Compact sets in the space* $L^p(0,T;B)$, Ann. Mat. Pura Appl, 1987, 146(4), 65-96.

[39] S. Sotoodeh Ghorbani, N. Taherpour, S. Bayat et al., *Epidemiologic characteristics of cases with reinfection, recurrence, and hospital readmission due to covid-19: A systematic review and meta-analysis*, Journal of medical virology, 2022, 94(1), 44-53.

[40] A. K. Srivastav, M. Ghosh, X.-Z. Li and L. Cai, *Modeling and optimal control analysis of covid-19: Case studies from italy and spain*, Mathematical Methods in the Applied Sciences, 2021, 44(11), 9210-9223.

[41] B. Tang, N. L. Bragazzi, Q. Li et al., *An updated estimation of the risk of transmission of the novel coronavirus (2019-ncov)*, Infectious disease modelling, 2020, 5, 248-255.

[42] S. Tian, N. Hu, J. Lou et al., *Characteristics of covid-19 infection in beijing*, Journal of infection, 2020, 80(4), 401-406.

[43] R. L. Tillett, J. R. Sevinsky, P. D. Hartley et al., *Genomic evidence for reinfection with sars-cov-2: a case study*, The Lancet infectious diseases, 2021, 21(1), 52-58.

[44] H. Tolley, D. Burdick, K. Manton and E. Stallard, *A compartment model approach to the estimation of tumor incidence and growth: Investigation of a model of cancer latency*, Biometrics, 1978, 377-389.

[45] S. Ullah and M. A. Khan, *Modeling the impact of non-pharmaceutical interventions on the dynamics of novel coronavirus with optimal control analysis with a case study*, Chaos, Solitons & Fractals, 2020, 139, 110075.

[46] S. Ullah, M. F. Khan, S. A. A. Shah et al., *Optimal control analysis of vector-host model with saturated treatment*, The European Physical Journal Plus, 2020, 135(10), 1-25.

[47] J. Wu, *Theory and applications of partial functional differential equations*, 119, Springer Science, 1996.

[48] H. Xin, Y. Li, P. Wu et al., *Estimating the latent period of coronavirus disease 2019 (covid-19)*, Clinical Infectious Diseases, 2022, 74(9), 1678-1681.

[49] Z. Zhang and R. K. Upadhyay, *Dynamical analysis for a deterministic svirs epidemic model with holling type ii incidence rate and multiple delays*, Results in Physics, 2021, 24, 104181.